TVNet: A novel time series analysis method based on dynamic convolution and 3D-Variation

Chenghan Li^{*1}**, Mingchen Li**^{*2} **& Ruisheng Diao**$^{\dagger 3}$
[1]Shenzhen International Graduate School(SIGS),Tsinghua University
[2]The Hong Kong University of Science and Technology (Guangzhou)
[3] †ZJU-UIUC Institute, Zhejiang University
lich24@mails.tsinghua.edu.cn; mli736@connect.hkust-gz.edu.cn;
ruishengdiao@intl.zju.edu.cn

Abstract

At present, the research on time series often focuses on the use of Transformer-based and MLP-based models.Conversely, the performance of Convolutional Neural Networks (CNNs) in time series analysis has fallen short of expectations, diminishing their potential for future applications. Our research aims to enhance the representational capacity of Convolutional Neural Networks (CNNs) in time series analysis by introducing novel perspectives and design innovations. To be specific, We introduce a novel time series reshaping technique that considers the inter-patch, intra-patch, and cross-variable dimensions. Consequently, we propose **TVNet**, **a dynamic convolutional network leveraging a 3D perspective to employ time series analysis**. TVNet retains the computational efficiency of CNNs and achieves state-of-the-art results in five key time series analysis tasks, offering a superior balance of efficiency and performance over the state-of-the-art Transformer-based and MLP-based models. Additionally, our findings suggest that TVNet exhibits enhanced transferability and robustness. Therefore, it provides a new perspective for applying CNN in advanced time series analysis tasks.

1 Introduction

Time series analysis plays a crucial role in many domains(Alfares & Nazeeruddin, 2002), such as anomaly detection(Pang et al., 2021) in industry signal and generation predication of renewable energy sources(Zhang et al., 2014). In recent years, remarkable progress has been made in this area(Wu et al., 2022a),(Luo & Wang, 2024). In particular, the MLP-based and Transformer-based architecture has been fully explored in the field of time series analysis (Wu et al., 2021),(Zhou et al., 2022),(Zhou et al., 2021),(Wu et al., 2022b),(Li et al., 2023a),(Challu et al., 2023). However, Transformers exhibit relatively low computational resource efficiency in time series tasks. MLP-based models often struggle to effectively capture the complex dependencies among variables and RNN-based models face challenges in modeling global temporal correlations. **In previous studies(Wang et al., 2024a), CNNs have been shown to be a neural network architecture that can balance efficiency and effectiveness. However, in the past, CNN architecture was often focused on video and images, and its application and research in time series predication and analysis are relatively limited.**

Time series data constitute records of continuous temporal changes, analogous to how video footage captures continuous visual transformations frame by frame - both capturing temporal continuity in their respective domains. Unlike certain sequential data types such as language(Lim & Zohren, 2021), time series data inherently reflect continuous phenomena. Much as a single video frame typically fails to convey the complete narrative of a scene, an isolated timestamp in a sequence usually lacks sufficient context for comprehensive analysis. This connection inspires us to leverage CNNs to

[*]Equal contribution.
[†]Corresponding author.

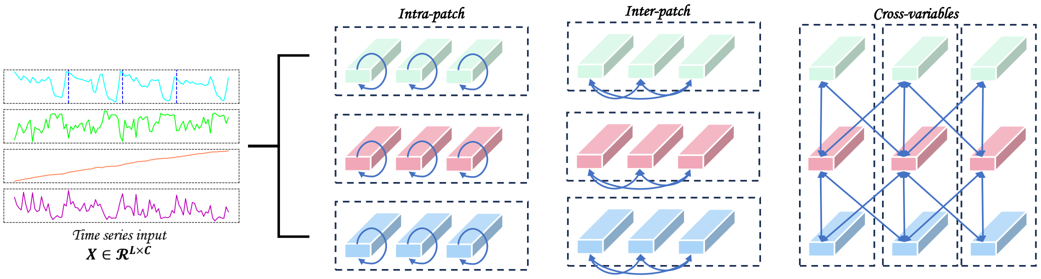

Figure 1: In the context of time series analysis, the three-dimensional variation encompasses **intra-patch**, **inter-patch**, and **cross-variable** interactions.

capture multiple dependencies(Lai et al., 2018; Luo & Wang, 2024), particularly the dynamic convolutions frequently employed in video processing, to attempt comprehensive capture of complex temporal patterns in time series data.

Modeling one-dimensional time variations can be a complex task due to the intricate patterns involved. Real-world time series often exhibit complex characteristics that require thorough analysis to interpret short-term fluctuations, long-term trends, and temporal pattern changes. Concurrently, the cross-variable dependencies within multivariate time series must be considered. To extract these crucial relationships from time series data, we specifically select intra-patch, inter-patch, and cross-variable(Figure 1) dependencies, derived from time series characteristics. These three types of embeddings encompass many significant information flows present in time series data.(Liang, 2014; Hlaváčková-Schindler et al., 2007)

Motivated by the above considerations, we introduce a novel analytical approach within the realm of time series analysis by integrating dynamic convolution. Specifically, we introduce a 3D-Embedding technique to convert one-dimensional time series tensors into three-dimensional tensors. Subsequently, we propose a network architecture, termed **TVNet (Time-Video Net)**, which leverages dynamic convolution to effectively capture intra-patch, inter-patch, and cross-variable dependencies for comprehensive time series analysis. We assessed the performance of TVNet across five benchmark analytical tasks: long-term and short-term forecasting, imputation, classification, and anomaly detection. Notably, despite being a purely convolution-based model, TVNet consistently achieves state-of-the-art results in these domains. Importantly, TVNet retains the efficiency inherent to dynamic convolution models, thereby achieving a superior balance between efficiency and performance, providing a practical and effective solution for time series analysis. **Our contributions are as follows:**

- A novel modeling approach that captures intra-patch,inter-patch and cross-variables features by converting 1D time series data into 3D shape tensor is proposed.
- TVNet implements consistent state-of-the-art performance time series analysis tasks across multiple mainstreams, demonstrating excellent task generalization.
- TVNet offers a better balance between efficiency and performance. It maintains the efficiency benefits of convolution based models while competing or even better with the most advanced base models in terms of performance.

2 Related Work

2.1 Time Series Analysis

Traditional time series analysis methods, such as ARIMA (Anderson, 1976) and Holt-Winters models (Hyndman, 2018), despite their solid theoretical underpinnings, are insufficient for datasets exhibiting intricate temporal patterns. In recent years, deep learning approaches, particularly MLP-based and Transformer-based models, have achieved significant advancements in this domain (Li et al., 2023a; Challu et al., 2023; Liu et al., 2021; Zhang & Yan, 2023; Zhou et al., 2022; Wu et al., 2021; Liu et al., 2023). MLP-based models have garnered increasing attention in time series analysis due to their low computational complexity. For instance, the Dlinear model (Li et al., 2023a) achieves efficient time series prediction by integrating decomposition techniques with MLP. However, current MLP models still struggle with capturing multi-period characteristics of time series and the relationship between different variables. Concurrently, Transformer-based models have demonstrated formidable performance in time series. Their self-attention mechanisms enable the capture of both long-term dependencies and critical global information. Nevertheless, their scalability and efficiency are constrained by the quadratic complexity of attention mechanisms. To mitigate this, researchers have introduced techniques to diminish the computational load of Transformers. For example, Pyraformer (Liu et al., 2021) enhances the model architecture with a pyramid attention design, facilitating connections across different scales. The recent PatchTST (Nie et al., 2022) employs a block-based strategy, enhancing both local feature capture and long-term prediction accuracy. Despite these innovations, existing Transformer-based methods, which predominantly model 1D temporal variations, continue to encounter substantial computational challenges in long-term time series analysis.

2.2 Convolution In Time Series Analysis

As deep learning techniques advance, Transformer-based and MLP-based models have achieved notable success in time series analysis, overshadowing traditional convolutional methods. Yet, innovative research is revitalizing convolution for time series analysis. The MICN model (Wang et al., 2023) integrates local features and global correlations by employing a multi-scale convolution structure. SCINet (Liu et al., 2022a) innovates by discarding causal convolution in favor of a recursive downsample-convolution interaction architecture to handle complex temporal dynamics. While these models have made strides in capturing long-term dependencies, they are challenged in the generality of time series tasks. TimesNet (Wu et al., 2022a) uniquely transforms one-dimensional time series into 2D forms, leveraging two-dimensional convolutional techniques from computer vision to enhance information representation. ModernTCN (Luo & Wang, 2024) extends the scope of convolutional technology by utilizing large convolution kernels to capture global time series features. However, these models predominantly focus on feature analysis within a single time window, neglecting the comprehensive integration of global, local, and cross-variable interactions.

2.3 Dynamic Convolution In Video

Dynamic convolution, characterized by their adaptive weight or module adjustments, exhibit structural flexibility in response to content variations. These networks incorporate dynamic filtering or convolution mechanisms ((Jia et al., 2016), (Yang et al., 2019)). They demonstrate superior processing capabilities and enhanced performance relative to conventional static networks. In the domain of video understanding, dynamic networks have also proven effective. For instance, dynamic filtering techniques and temporal aggregation methods adeptly capture temporal dynamics within videos, thereby augmenting the models' capacity to represent time series data.((Meng et al., 2021), (Li et al., 2020))

3 TVNet

Based on the inter-patch, intra-patch, and cross-variable features of the time series mentioned above, this paper proposes TVNet to capture the features of the time series. Specifically, we first design the 3D-embedding module so that the 1D time series can be converted to 3D time series tensor, and a 3D-block is designed to model the three types of properties (inter-patch,intra-patch, and cross-variable) through dynamic convolution. Finally, time series representations are extracted by 3D-blocks to get different task outputs through the linear layer. Figure 2 shows the structure of TVNet.

3.1 3D-Embedding

In this section, we propose a unique embedding way(**3D-Embedding**). This method takes into account the inter-patch, intra-patch and cross-variable for time series.We denote $X_{\text{in}} \in \mathbb{R}^{L\times C}$,$L$ means the length of time series,C means the dimensions of time series.

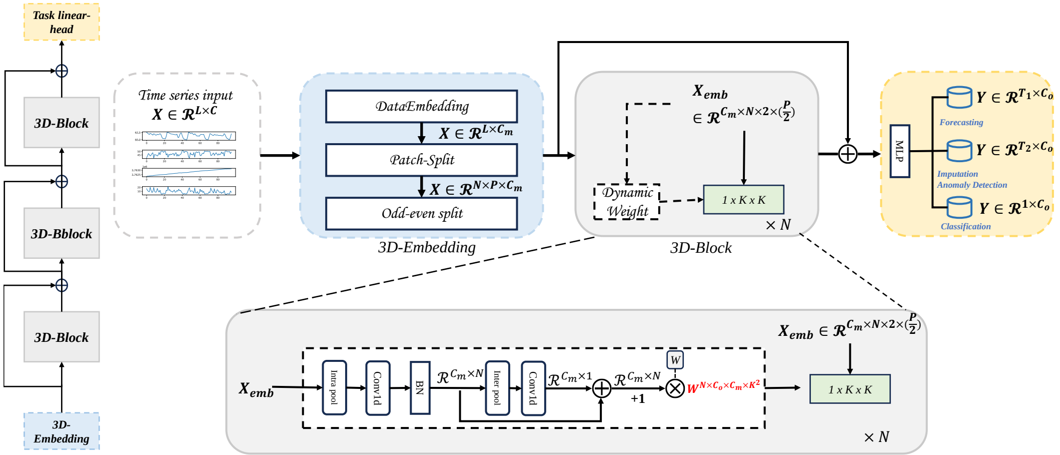
Task linear-head
3D-Block
3D-Bblock
3D-Block
3D-Embedding
Time series input
$X \in \mathcal{R}^{L\times C}$
DataEmbedding
$X \in \mathcal{R}^{L\times C_m}$
Patch-Split
$X \in \mathcal{R}^{N\times P\times C_m}$
Odd-even split
3D-Embedding
X_{emb}
$\in \mathcal{R}^{C_m\times N\times 2\times(\frac{P}{2})}$
Dynamic Weight
1 x K x K
× N
3D-Block
MLP
$Y \in \mathcal{R}^{T_1\times C_o}$
Forecasting
$Y \in \mathcal{R}^{T_2\times C_o}$
Imputation
Anomaly Detection
$Y \in \mathcal{R}^{1\times C_o}$
Classification
$X_{emb} \in \mathcal{R}^{C_m\times N\times 2\times(\frac{P}{2})}$
X_{emb}
Intra pool
Conv1d
BN
$\mathcal{R}^{C_m\times N}$
Inter pool
Conv1d
$\mathcal{R}^{C_m\times 1}$
$\mathcal{R}^{C_m\times N}$
+1
W
$W^{N\times C_o\times C_m\times K^2}$
1 x K x K
× N

Figure 2: The overarching architecture of **TVNet** is constructed by stacking 3D-blocks in a residual way, which enables the capture of inter-patch, intra-patch, and cross-variable features from the time series 3D tensor.

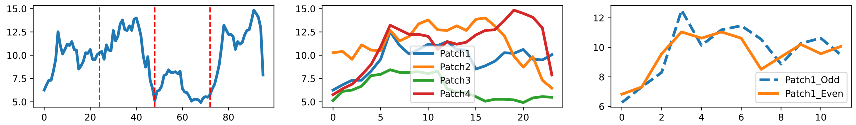

Figure 3: A univariate time series example is segmented into four distinct patches and the odd and even components specifically for Patch1 (ETTh1).

We first embed the input along the feature dimensions C to C_m and get $X_{\text{in}} \in \mathbb{R}^{L\times C_m}$, where C_m as the embedding dimensions.Embedding dimension C_m is a crucial hyperparameter that dictates the dimensionality of the representation space into which each time point is projected. After embedding the input data along the feature dimension to obtain $X_{\text{in}} \in \mathbb{R}^{L\times C_m}$, we proceed to segment the embedded data into patches using a one-dimensional convolutional layer (Conv1D). Specifically, we configure the Conv1D layer with a kernel size P, which defines the length of each patch. This configuration allows the Conv1D layer to divide the input sequence into N patches, where N is calculated based on the total length L, the patch length P(In the absence of overlapping patches,$N = L/P$). The output of this Conv1D operation is a tensor $X_{\text{emb}} \in \mathbb{R}^{N\times P\times C_m}$, with each N representing the number of patches, P representing the length of each patch, and C_m representing the embedding dimensions.Then we use odd-even split(Liu et al., 2022a) on the patch length demisions to get X_{odd} and $X_{even} \in \mathbb{R}^{N\times(P/2)\times C_m}$, then stacking X_{odd} and X_{even} to get $X_{\text{emb}} \in \mathbb{R}^{N\times 2\times(P/2)\times C_m}$. Figure 3 illustrates an example of patches and odd-even components applied to a univariate time series.(**see Algorithm** 2)

$$X_{\text{emb}} = \text{3D-Embedding}(X_{\text{in}}) \tag{1}$$

3.2 3D-BLOCK

Time dynamic weight: Previous research, as detailed in Wang et al. (2023), has highlighted both consistencies and discrepancies within time series data, particularly in the phenomenon known as mode drift.In response to these observations and inspired by dynamic convolution work in the video field(Huang et al., 2021), Regarding the 3D-Embedding technique mentioned earlier, we employ a dynamic convolutional method to capture the temporal dynamics within each patch. To clarify, the embedded representation X_{emb} is envisioned as a collection of individual patches, denoted as $(x_1, x_2, \ldots, x_N)$. The weight associated with the i-th patch, denoted as W_i, is hypothesized to be decomposable into the product of a constant **time base weight** $\boldsymbol{W_b}$, which is common across all patches, and a **time varying weight** $\boldsymbol{\alpha_i}$, which is unique to each patch.

$$\tilde{x}_i = \boldsymbol{W_i} \cdot x_i = (\boldsymbol{\alpha_i} \cdot \boldsymbol{W_b}) \cdot x_i, \tag{2}$$

Time varying weight generation: To more accurately model the temporal dynamics of patches, the time-varying weight α_i must account for all patches. Based on the above starting point, we design an adaptive Time-varying weight generation that fully considers the interaction between inter-patch and intra-patch.It can be articulated as $\alpha_i = \mathcal{G}(X_{\text{emb}})$. Here, $\mathcal{G}$ denotes the generation function for the time-varying weight.To efficiently handle both inter-patch and intra-patch relationships and to manage pre-training weights effectively, the weights of the 3D-block can be initialized akin to standard convolutional layers. This initialization is realized by setting the weights of $\mathcal{F}(\mathbf{v}_{\text{inter}}) + \mathcal{F}(\mathbf{v}_{\text{intra}})$ and augmenting the formulation with a constant vector of ones(1).The Figure 4 shows the flow chart for Time varing weight generation.

$$\alpha_i = \mathcal{G}(X_{\text{emb}}) = 1 + \mathcal{F}(\mathbf{v}_{\text{inter}}) + \mathcal{F}(\mathbf{v}_{\text{intra}}) \tag{3}$$

In this way, at the initial state,$W_i = 1 \cdot W_b$.

The function $\mathcal{F}(\mathbf{v}_{\text{intra}})$ captures intra-patch features. Initially, we apply 3D Adaptive Average Pooling to the embedded representation X_{emb} to obtain intra-patch description vectors $\mathbf{v}_{\text{intra}}$, which encapsulate the essential features of each patch. These vectors are of dimension $\mathbb{R}^{C_m \times N}$. This operation is described by the following equation:

$$\mathbf{v}_{\text{intra}} = \text{AdaptiveAvgPool3d}(X_{\text{emb}}) \tag{4}$$

Subsequently, for intra-patch channel modeling, we employ a single-layer Conv1D, denoted as $\mathcal{F}_{\text{intra}}$, on $\mathbf{v}_{\text{intra}}$.

$$\mathcal{F}_{\text{intra}}(\mathbf{v}_{\text{intra}}) = \delta(\text{BN}(\text{Conv1D}^{C \to C}(\mathbf{v}_{\text{intra}}))) \tag{5}$$

Here, δ represents ReLU activation, and BN denotes Batch Normalization.

The function $\mathcal{F}(\mathbf{v}_{\text{inter}})$ is tasked with capturing features for inter-patches. We employ Adaptive Average Pooling 1D on $\mathbf{v}_{\text{intra}}$ to derive $\mathbf{v}_{\text{inter}}$. This process can be expressed as:

$$\mathbf{v}_{\text{inter}} \in \mathbb{R}^{C_m \times 1} = \text{AdaptiveAvgPool1d}(\mathbf{v}_{\text{intra}}) \tag{6}$$

Subsequently, for inter-patch channel modeling, a single-layer Conv1D, denoted as $\mathcal{F}_{\text{inter}}$, is applied to $\mathbf{v}_{\text{inter}}$:

$$\mathcal{F}_{\text{inter}}(\mathbf{v}_{\text{inter}}) = \delta(\text{Conv1D}^{C \to C}(\mathbf{v}_{\text{inter}})) \tag{7}$$

Here, δ denotes the ReLU activation function.

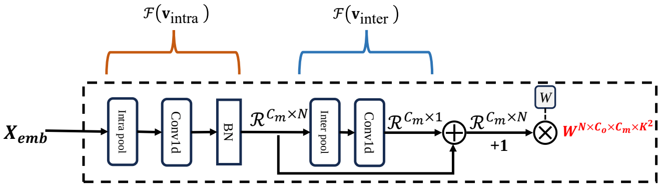
$\mathcal{F}(\mathbf{v}_{\text{intra}})$
$\mathcal{F}(\mathbf{v}_{\text{inter}})$
X_{emb}
Intra pool
Conv1d
BN
$\mathcal{R}^{C_m \times N}$
Inter pool
Conv1d
$\mathcal{R}^{C_m \times 1}$
$\mathcal{R}^{C_m \times N}$
+1
W
$W^{N \times C_o \times C_m \times K^2}$

Figure 4: The Time varying weight generation flow chart

3.3 Overall Structure

Following the 3D-Embedding process, the embedded representation X_{emb} can be permuted to the form $X_{\text{emb}} \in \mathbb{R}^{C_m \times N \times 2 \times (P/2)}$, which is then input into the 3D-block architecture. The purpose of this step is to learn effective representations of the time series, denoted as $X^{3D} \in \mathbb{R}^{C_m \times N \times 2 \times (P/2)}$. Subsequently, X^{3D} is reshaped into $X \in \mathbb{R}^{(NP) \times C_m}$ and passed through linear layer, also referred to as the task-linear head, to accommodate the specific requirements of various tasks.

$$X^{3D} = \text{TVNet}(X_{\text{emb}}) \tag{8}$$

TVNet($\cdot$) is the stacked 3D-blocks. Each 3D-block is organized in a residual way. The forward process in the i-th 3D block is:

$$X^{3D}_{i+1} = \text{3D-block}(X^{3D}_i) + X^{3D}_i \tag{9}$$

where $X^{3D}_i \in \mathbb{R}^{C_m \times N \times 2 \times (P/2)}$ is the i-th block's input.((**see Algorithm** 1))

Algorithm 1 Training of TVNet.

```
Require: Input: Training set $\mathcal{D} = \{(X, Y)\}$ Look back window $X \in \mathbb{R}^{L \times C}$;Embedding dimensions $C_m$;number of 3D-blocks $L$;Patch length$P$ and other training hyperparameter.
Ensure: Output: Trained TVNet
Initialize Embedding dimensions and number of 3D-blocks.
Sample $(X, Y)$ from $\mathcal{D}$
(3D-Embdding): $X_{emb} = Algorithm(X)$
for for $i$ 1 to $L$ do: do
    $\alpha \leftarrow \mathcal{G}(X_{emb})$
    $X_i^{3D} \leftarrow Conv2D(\alpha, W_b, X_{i-1}^{3D})$
end for
$\hat{Y} \leftarrow$ Task linear head$(X^{3D})$
Compute loss $\mathcal{L} \leftarrow \mathcal{L}(\hat{Y}, Y)$
Update model parameters $\Theta$ via backpropagation
until convergence
return Trained TVNet
```

4 Experiment

TVNet is evaluated across five common analytical tasks, including both long-term and short-term forecasting, data imputation, classification, and anomaly detection, to demonstrate its adaptability in diverse applications.

Baselines: In establishing foundational models for time series analysis, we have extensively incorporated the most recent and advanced models from the time series community as benchmarks. This includes Transformer-based models such as iTransformer, PatchTST, Crossformer, and FEDformer(Liu et al., 2023; Nie et al., 2022; Zhang & Yan, 2023; Zhou et al., 2022); MLP-based models like MTS-Mixer, Dlinear RMLP, and RLinear(Li et al., 2023b; Zeng et al., 2023; Li et al., 2023a); and Convolution-based models including TimesNet, MICN, and ModernTCN(Wu et al., 2022a; Wang et al., 2023; Luo & Wang, 2024). Additionally, we have included state-of-the-art models from each specific task to serve as supplementary benchmarks for a comprehensive comparison. Our objective is to ensure that our model exhibits competitiveness when benchmarked against these advanced models.

Hyperparameter Setups: The performance of a model can be influenced by various hyperparameter settings. In this study, the hyperparameter ranges for TVNet are aligned with those reported in Wu et al. (2022a). A detailed discussion on the impact of each hyperparameter is provided in **Appendices C and D.**

Main results: As depicted in Figure 5, **TVNet consistently achieves top-tier performance across five pivotal analytical tasks, showcasing enhanced efficiency.** A detailed analysis of the experi-

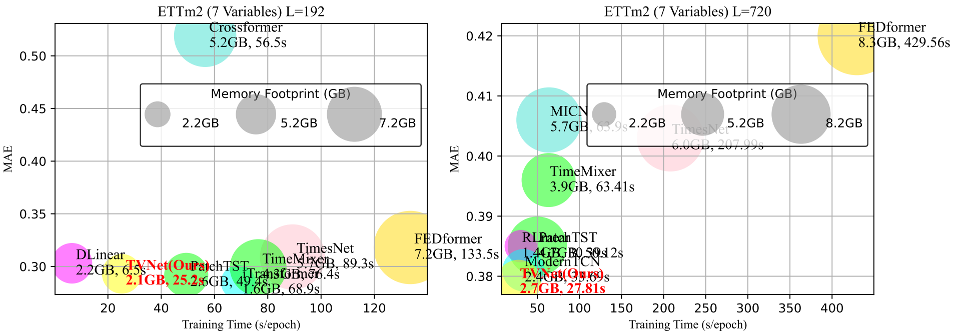

Figure 5: Model efficiency comparison under the setting of L(prediction length) =192/720 of ETTm2.

mental results is presented in Section 5.1. The details and outcomes of the experiments for each task are discussed in the following subsections. In the tables, the superior results are highlighted in **bold**, while those ranking just below the top are indicated with underlined.

4.1 Long-term forecasting

Datasets and setups: We performed long-term forecasting experiments on nine well-established real-world benchmarks: Weather(wet), Traffic(pem), Electricity(uci), Exchange(Lai et al., 2018), ILI(cdc), and four ETT datasets(Zhou et al., 2021). To ensure equitable comparison, we re-executed all baseline models with diverse input lengths, opting for the best outcomes to prevent underestimating their performance. Mean Squared Error (MSE) and Mean Absolute Error (MAE) are adopted as the metrics for evaluating multivariate time series forecast.

Results: Table 1 illustrates the exceptional performance of TVNet in long-term forecasting. Specifically, TVNet outperformed the majority of existing MLP-based, Transformer-based, and Convolution-based models across all nine datasets. This outcome suggests that our design significantly improves the predictive capabilities of time series forecasting via convolution.

Table 1: Long-term forecasting results are averaged across four prediction lengths: {*24*, *36*, *48*, *60*} for ILI and {*96*, *192*, *336*, *720*} for others. Lower MSE or MAE values indicate superior performance. Refer to Table 28 in the Appendix for comprehensive results.(Hint:Baseline results are derived from their papers)

Models		**TVNet** (Ours)		PatchTST (2022)		iTransformer (2023)		Crossformer (2023)		RLinear (2023a)		MTS-Mixer (2023b)		DLinear (2023b)		TimesNet (2022a)		MICN (2023)		ModernTCN (2024)		FEDformer (2022)		RMLP (2023a)	
Metrics		MSE	MAE	MSE	MAE	MSE	MAE	MSE	MAE	MSE	MAE	MSE	MAE	MSE	MAE	MSE	MAE	MSE	MAE	MSE	MAE	MSE	MAE	MSE	MAE
ETTm1	Avg	**0.348**	**0.379**	0.351	0.381	0.407	0.410	0.431	0.443	0.358	0.376	0.370	0.395	0.357	0.379	0.400	0.450	0.383	0.406	0.351	0.381	0.382	0.422	0.369	0.393
ETTm2	Avg	**0.251**	**0.311**	0.255	0.315	0.288	0.332	0.632	0.578	0.256	0.314	0.277	0.325	0.267	0.332	0.291	0.333	0.277	0.336	0.253	0.314	0.292	0.343	0.268	0.322
ETTh1	Avg	0.407	0.421	0.413	0.431	0.454	0.447	0.441	0.465	0.408	0.421	0.430	0.436	0.423	0.437	0.458	0.450	0.433	0.462	**0.404**	**0.420**	0.428	0.454	0.442	0.445
ETTh2	Avg	0.324	0.377	0.330	0.379	0.383	0.407	0.835	0.676	**0.320**	**0.378**	0.386	0.413	0.431	0.447	0.414	0.427	0.385	0.430	0.322	0.379	0.388	0.434	0.349	0.395
Electricity	Avg	0.165	0.254	0.159	**0.253**	0.178	0.270	0.293	0.351	0.169	0.261	0.173	0.272	0.177	0.274	0.192	0.295	0.182	0.292	**0.156**	**0.253**	0.207	0.321	0.161	**0.253**
Weather	Avg	**0.221**	**0.261**	0.226	0.264	0.258	0.278	0.230	0.290	0.247	0.279	0.235	0.272	0.240	0.300	0.259	0.287	0.242	0.298	0.224	0.264	0.310	0.357	0.225	0.265
Traffic	Avg	0.396	0.268	**0.391**	**0.264**	0.428	0.282	0.535	0.300	0.518	0.383	0.494	0.354	0.434	0.295	0.620	0.336	0.535	0.312	0.396	0.270	0.604	0.372	0.466	0.348
Exchange	Avg	0.298	0.367	0.387	0.419	0.360	0.403	0.701	0.633	0.345	0.394	0.373	0.407	**0.297**	0.378	0.416	0.443	0.315	0.404	0.302	**0.366**	0.478	0.478	0.345	0.394
ILI	Avg	**1.406**	**0.766**	1.443	0.798	2.141	0.996	3.361	1.235	4.269	1.490	1.555	0.819	2.169	1.041	2.139	0.931	2.567	1.055	1.440	0.786	2.597	1.070	4.387	1.516

4.2 Short-term forecasting

Datasets and setups: Our benchmark for short-term forecasting is the M4 dataset, as introduced by Makridakis (Makridakis et al., 2018). We have set the input sequence length to be twice that of the forecast horizon(Wu et al., 2022a). For evaluating performance, we utilize key metrics including the Symmetric Mean Absolute Percentage Error (SMAPE), Mean Absolute Scaled Error (MASE), and Overall Weighted Average (OWA). To enhance our comparative analysis, we have incorporated models such as U-Mixer (Ma et al., 2024) and N-Hits (Challu et al., 2023).

Results: Table 2 presents the findings. The short-term forecasting task on the M4 dataset is notably challenging due to the varied sources and temporal dynamics of the time series data. Nevertheless, TVNet retains its top ranking in this rigorous context, demonstrating its enhanced ability for temporal analysis.

Table 2: The task of short-term forecasting entails evaluating performance across various sub-datasets, each with distinct sampling intervals. The results are presented as a weighted average, with lower metric values signifying enhanced performance. Full results are provided in Table 29

Models		**TVNet** (Ours)	PatchTST (2022)	U-Mixer (2024)	Crossformer (2023)	RLinear (2023a)	MTS-Mixer (2023b)	DLinear (2023b)	TimesNet (2022a)	MICN 2023)	ModernTCN (2024)	FEDformer (2022)	N-HiTS (2023)
WA	SMAPE	**11.671**	11.807	11.740	13.474	12.473	11.892	13.639	11.829	13.130	11.698	12.840	11.927
	MSE	**1.536**	1.590	1.575	1.866	1.677	1.608	2.095	1.585	1.896	11.556	1.701	1.613
	OWA	**0.832**	0.851	0.845	0.985	0.898	0.859	1.051	0.851	0.980	0.838	0.918	0.861

4.3 IMPUTATION

Datasets and setups: The imputation task is designed to estimate missing values within partially observed time series data. Missing values are prevalent in time series due to unforeseen incidents such as equipment failure or communication errors. Given that missing values can adversely affect the performance of subsequent analyses, the imputation task holds significant practical importance.(Wu et al., 2022a) Subsequently, we concentrate on electricity and weather scenarios, which frequently exhibit data loss issues. We have chosen datasets from these domains as benchmarks, including ETT(Zhou et al., 2021), Electricity (UCI)(uci), and Weather(wet). To assess the model's capacity under varying degrees of missing data, we randomly introduce data occlusions at ratios of {*12.5%*, *25%*, *37.5%*, *50%*}.

Results: Table 3 shows TVNet's strong imputation performance despite irregular observations due to missing values. TVNet's top results validate its capability to capture temporal dependencies in complex scenarios. Cross-variable dependencies are key in imputation, aiding in estimating missing values when some variables are observed. Methods ignoring these, like PatchTST(Nie et al., 2022) and DLinear(Zeng et al., 2023), perform poorly in this task.

Table 3: Average results for the imputation task. Randomly masking {*12.5%*, *25%*, *37.5%*, *50%*} time points to compare the model performance under different missing degrees.Full results can be seen in 30

Models		**TVNet** (Ours)		PatchTST (2022)		SCINet (2022a)		Crossformer (2023)		RLinear (2023a)		MTS-Mixer (2023b)		DLinear (2023)		TimesNet (2022a)		MICN 2023)		ModernTCN (2024)		FEDformer (2022)		RMLP (2023a)	
Metrics		MSE	MAE	MSE	MAE	MSE	MAE	MSE	MAE	MSE	MAE	MSE	MAE	MSE	MAE	MSE	MAE	MSE	MAE	MSE	MAE	MSE	MAE	MSE	MAE
ETTm1	Avg	**0.018**	**0.088**	0.045	0.133	0.039	0.129	0.041	0.143	0.070	0.166	0.056	0.154	0.093	0.206	0.027	0.107	0.070	0.182	0.020	0.093	0.062	0.177	0.063	0.161
ETTm2	Avg	0.022	0.086	0.028	0.098	0.027	0.102	0.046	0.149	0.032	0.108	0.032	0.107	0.096	0.208	0.022	0.088	0.144	0.249	**0.019**	**0.082**	0.101	0.215	0.032	0.109
ETTh1	Avg	**0.046**	**0.145**	0.133	0.236	0.104	0.216	0.132	0.251	0.141	0.242	0.127	0.236	0.201	0.306	0.078	0.187	0.125	0.250	0.050	0.150	0.117	0.246	0.134	0.239
ETTh2	Avg	**0.039**	**0.127**	0.066	0.164	0.064	0.165	0.122	0.240	0.066	0.165	0.069	0.168	0.142	0.259	0.049	0.146	0.205	0.307	0.042	0.131	0.163	0.279	0.068	0.166
Electricity	Avg	0.079	0.194	0.091	0.209	0.086	0.201	0.083	0.199	0.119	0.246	0.089	0.208	0.132	0.260	0.092	0.210	0.119	0.247	**0.073**	**0.187**	0.130	0.259	0.099	0.221
Weather	Avg	**0.024**	**0.039**	0.033	0.057	0.031	0.053	0.036	0.090	0.034	0.058	0.036	0.058	0.052	0.110	0.030	0.054	0.056	0.128	0.027	0.044	0.099	0.203	0.035	0.060

4.4 CLASSIFICATION AND ANOMALY DETECTION

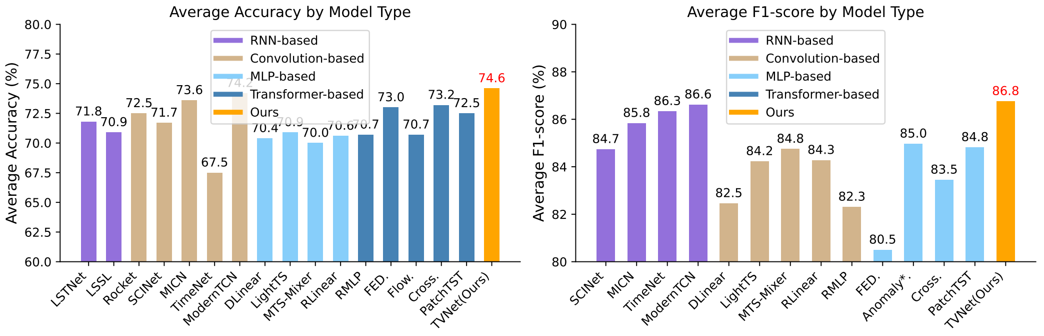

Figure 6: The results are averaged from several datasets.Higher accuracy and F1 score indicate better performance. * in the Transformer-based models indicates the name of *former. See Table 31 and 32 in Appendix for full results.

Datasets and setups: In our classification study, we selected 10 multivariate datasets from the UEA Time Series Classification Archive, as introduced by Bagnall (Bagnall et al., 2018) in 2018. These datasets, which serve as benchmarks, have been standardized using pre-processing practices established by Wu(Wu et al., 2022a). To ensure a comprehensive comparison, we have integrated state-of-the-art methods, including LSTNet (Lai et al., 2018), Rocket (Dempster et al., 2020), and Flowformer (Wu et al., 2022b), into our evaluation framework.

Our analysis covers a range of established benchmarks in the field of anomaly detection, including SMD (Su et al., 2019), SWaT (Mathur & Tippenhauer, 2016), PSM (Abdulaal et al., 2021), MSL, and SMAP (Hundman et al., 2018). To enhance our comparative analysis, we have incorporated the Anomaly Transformer (Xu et al., 2021) into our baseline models. Our methodology is based on the traditional approach of reconstruction, wherein the deviation from the original, measured by the reconstruction error, is the key indicator for detecting anomalies.

Results: The results for time series classification and anomaly detection are depicted in Figure 6. In the classification task, TVNet attained the highest performance, with an average accuracy of 74.6%. For the anomaly detection task, TVNet exhibited competitive results 86.8 relative to the previous state-of-the-art.

5 Model Analysis

5.1 Comprehensive comparison of performance and efficiency

Summary of results: Relative to other task-specific models and prior state-of-the-art benchmarks, TVNet has consistently achieved state-of-the-art performance across five key analytical tasks, highlighting its exceptional versatility for diverse mission types. Moreover, TVNet's efficiency, as illustrated in Figure 5, facilitates a superior balance between efficiency and performance.

Compared with baselines: TVNet outperforms both Transformer-based and MLP-based models in terms of performance. Concurrently, it achieves faster training speeds and lower memory usage compared to Transformer-based models, thereby demonstrating superior efficiency. TVNet's comprehensive consideration of the relationships among time series inter-patch, intra-patch, and cross-variables enhances its representational capacity over the lightweight backbone of MLP models. Compared to ModernTCN, MICN, and TimesNet, TVNet employs dynamic convolution and 3D-Embedding techniques, significantly enhancing its memory efficiency and training speed while achieving the best possible results.

Analysis of complexity: TVNet exhibits a time complexity of $O(LC_m^2)$ and a space complexity of $O(C_m^2)$, where C_m denotes the embedding dimension. A comparison of time complexity and memory usage during training and inference phases is presented in Table 4. Relative to Transformer-based models, TVNet demonstrates lower time complexity, and in contrast to convolutional models, it maintains independence between space complexity and sequence length.

Table 4: Comparison of different methods in terms of training time and memory complexity.

Methods	Time Complexity	Space complexity
TVNet (Ours)	$O(LC_m^2)$	$O(C_m^2 + LC_m)$
MICN(Wang et al., 2023)	$O(LC_m^2)$	$O(LC_m^2)$
FEDformer(Zhou et al., 2022)	$O(L)$	$O(L)$
Autoformer(Wu et al., 2021)	$O(L \log L)$	$O(L \log L)$
Informer(Zhou et al., 2021)	$O(L \log L)$	$O(L \log L)$
Transformer(Liu et al., 2023)	$O(L^2)$	$O(L^2)$
LSTM	$O(L)$	$O(L)$

5.2 Ablation analysis

Ablation of inter-pool module: We conducted ablation experiments on the inter-pool module, and the experimental results are shown in the Table 5. It is found in the table that when inter-pool is removed, the predicted results will decrease, indicating that inter-pool can increase the representation of the relationship between different patches.

Ablation of dynamic convolution: Comparing the dynamic convolution weights to their fixed counterparts reveals a significant decline in predictive performance without the former. This observation underscores the effectiveness of the context-aware dynamic convolution proposed in this paper for modeling time series analysis.(Table 6) The dynamic convolution mechanism allows for a more nuanced capture of complex temporal patterns, enhancing the model's ability to adapt to varying data distributions and nonlinear relationships.

Table 5: Ablation of inter-pool module in the TVNet.w/o means without module.

Models	Metrics	Weather				Electricity				Traffic			
		96	192	336	720	96	192	336	720	96	192	336	720
TVNet	MSE	0.147	0.194	0.235	0.308	0.142	0.165	0.164	0.190	0.367	0.381	0.395	0.442
	MAE	0.198	0.238	0.277	0.331	0.223	0.241	0.269	0.284	0.252	0.262	0.268	0.290
w/o inter-pool	MSE	0.156	0.211	0.247	0.349	0.147	0.178	0.186	0.199	0.377	0.399	0.410	0.458
	MAE	0.212	0.276	0.303	0.375	0.229	0.251	0.276	0.302	0.276	0.284	0.301	0.328

Table 6: Ablation of dynamic convolution in the TVNet.w/o means without module.

Models	Metrics	Weather				Electricity				Traffic			
		96	192	336	720	96	192	336	720	96	192	336	720
TVNet	MSE	**0.147**	**0.194**	**0.235**	**0.308**	**0.142**	**0.165**	**0.164**	**0.190**	**0.367**	**0.381**	**0.395**	**0.442**
	MAE	**0.198**	**0.238**	**0.277**	**0.331**	**0.223**	**0.241**	**0.269**	**0.284**	**0.252**	**0.262**	**0.268**	**0.290**
w/o dynamic weight	MSE	0.251	0.257	0.291	0.341	0.185	0.201	0.214	0.268	0.391	0.423	0.440	0.507
	MAE	0.226	0.269	0.301	0.370	0.275	0.296	0.308	0.316	0.306	0.313	0.311	0.327

5.3 Transfer learning

Figures 7 and 8 illustrate the outcomes of our transfer learning experiments. In both direct prediction and full-tuning approaches, TVNet outperforms the baseline models, underscoring its superior generalization and transfer capabilities. A pivotal advantage of TVNet is its dynamic weighting mechanism, which adeptly captures intricate temporal dynamics across a variety of datasets.

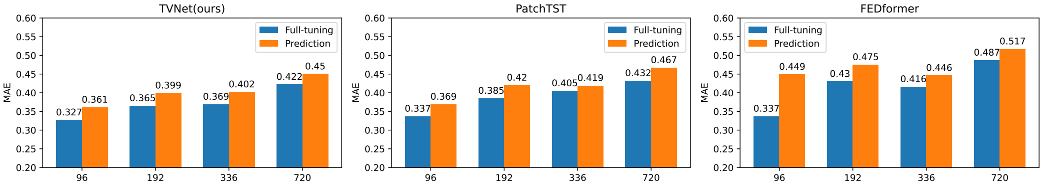

Figure 7: Transfer learning results for ETTh2.

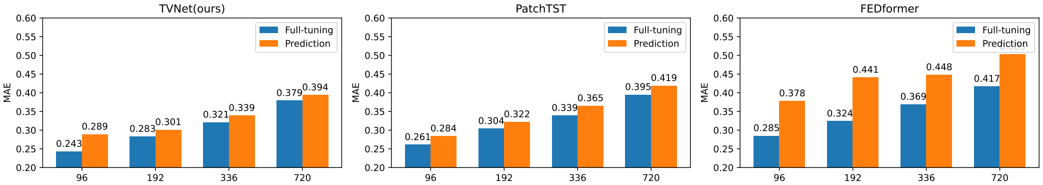

Figure 8: Transfer learning results for ETTm2.

6 Conclusion and Future Work

This paper introduces a 3D variational reshaping and dynamic convolution method for general time series analysis. The experimental results demonstrate that TVNet exhibits excellent versatility across tasks, achieving performance comparable to or surpassing that of the most advanced Transformer-based and MLP-based models. TVNet also preserves the efficiency inherent in Convolution-based models, thus providing an optimal balance between performance and efficiency. Future research will focus on large-scale pre-training methods for time series and multi-scale patches, leveraging TVNet as the foundational architecture, which is anticipated to enhance capabilities across a broad spectrum of downstream tasks.

References

Cdc. illness. URL `https://gis.cdc.gov/grasp/fluview/fluportaldashboard.html`. Accessed: 2024-08-10.

Pems. traffic. URL http://pems.dot.ca.gov/. Accessed: 2024-08-10.

Uci. electricity. URL https://archive.ics.uci.edu/ml/datasets/ElectricityLoadDiagrams20112014. Accessed: 2024-08-10.

Wetterstation. weather. URL https://www.bgc-jena.mpg.de/wetter/. Accessed: 2024-08-10.

Ahmed Abdulaal, Zhuanghua Liu, and Tomer Lancewicki. Practical approach to asynchronous multivariate time series anomaly detection and localization. In *Proceedings of the 27th ACM SIGKDD conference on knowledge discovery & data mining*, pp. 2485–2494, 2021.

Hesham K Alfares and Mohammad Nazeeruddin. Electric load forecasting: literature survey and classification of methods. *International journal of systems science*, 33(1):23–34, 2002.

Oliver D Anderson. Time-series. 2nd edn., 1976.

Anthony Bagnall, Hoang Anh Dau, Jason Lines, Michael Flynn, James Large, Aaron Bostrom, Paul Southam, and Eamonn Keogh. The uea multivariate time series classification archive, 2018. *arXiv preprint arXiv:1811.00075*, 2018.

Cristian Challu, Kin G Olivares, Boris N Oreshkin, Federico Garza Ramirez, Max Mergenthaler Canseco, and Artur Dubrawski. Nhits: Neural hierarchical interpolation for time series forecasting. In *Proceedings of the AAAI conference on artificial intelligence*, volume 37, pp. 6989–6997, 2023.

Angus Dempster, François Petitjean, and Geoffrey I Webb. Rocket: exceptionally fast and accurate time series classification using random convolutional kernels. *Data Mining and Knowledge Discovery*, 34(5):1454–1495, 2020.

Albert Gu, Karan Goel, and Christopher Ré. Efficiently modeling long sequences with structured state spaces. *arXiv preprint arXiv:2111.00396*, 2021.

Katerina Hlaváčková-Schindler, Milan Paluš, Martin Vejmelka, and Joydeep Bhattacharya. Causality detection based on information-theoretic approaches in time series analysis. *Physics Reports*, 441(1):1–46, 2007.

Ziyuan Huang, Shiwei Zhang, Liang Pan, Zhiwu Qing, Mingqian Tang, Ziwei Liu, and Marcelo H Ang Jr. Tada! temporally-adaptive convolutions for video understanding. *arXiv preprint arXiv:2110.06178*, 2021.

Kyle Hundman, Valentino Constantinou, Christopher Laporte, Ian Colwell, and Tom Soderstrom. Detecting spacecraft anomalies using lstms and nonparametric dynamic thresholding. In *Proceedings of the 24th ACM SIGKDD international conference on knowledge discovery & data mining*, pp. 387–395, 2018.

RJ Hyndman. *Forecasting: principles and practice*. OTexts, 2018.

Furong Jia, Kevin Wang, Yixiang Zheng, Defu Cao, and Yan Liu. Gpt4mts: Prompt-based large language model for multimodal time-series forecasting. In *Proceedings of the AAAI Conference on Artificial Intelligence*, volume 38, pp. 23343–23351, 2024.

Xu Jia, Bert De Brabandere, Tinne Tuytelaars, and Luc V Gool. Dynamic filter networks. *Advances in neural information processing systems*, 29, 2016.

Ming Jin, Shiyu Wang, Lintao Ma, Zhixuan Chu, James Y Zhang, Xiaoming Shi, Pin-Yu Chen, Yuxuan Liang, Yuan-Fang Li, Shirui Pan, et al. Time-llm: Time series forecasting by reprogramming large language models. *arXiv preprint arXiv:2310.01728*, 2023.

Diederik P Kingma. Adam: A method for stochastic optimization. *arXiv preprint arXiv:1412.6980*, 2014.

Guokun Lai, Wei-Cheng Chang, Yiming Yang, and Hanxiao Liu. Modeling long-and short-term temporal patterns with deep neural networks. In *The 41st international ACM SIGIR conference on research & development in information retrieval*, pp. 95–104, 2018.

Yunsheng Li, Yinpeng Chen, Xiyang Dai, Dongdong Chen, Mengchen Liu, Lu Yuan, Zicheng Liu, Lei Zhang, and Nuno Vasconcelos. Micronet: Towards image recognition with extremely low flops. *arXiv preprint arXiv:2011.12289*, 2020.

Zhe Li, Shiyi Qi, Yiduo Li, and Zenglin Xu. Revisiting long-term time series forecasting: An investigation on linear mapping. *arXiv preprint arXiv:2305.10721*, 2023a.

Zhe Li, Zhongwen Rao, Lujia Pan, and Zenglin Xu. Mts-mixers: Multivariate time series forecasting via factorized temporal and channel mixing. *arXiv preprint arXiv:2302.04501*, 2023b.

X San Liang. Unraveling the cause-effect relation between time series. *Physical Review E*, 90(5): 052150, 2014.

Bryan Lim and Stefan Zohren. Time-series forecasting with deep learning: a survey. *Philosophical Transactions of the Royal Society A*, 379(2194):20200209, 2021.

Minhao Liu, Ailing Zeng, Muxi Chen, Zhijian Xu, Qiuxia Lai, Lingna Ma, and Qiang Xu. Scinet: Time series modeling and forecasting with sample convolution and interaction. *Advances in Neural Information Processing Systems*, 35:5816–5828, 2022a.

Shizhan Liu, Hang Yu, Cong Liao, Jianguo Li, Weiyao Lin, Alex X Liu, and Schahram Dustdar. Pyraformer: Low-complexity pyramidal attention for long-range time series modeling and forecasting. In *International conference on learning representations*, 2021.

Yong Liu, Haixu Wu, Jianmin Wang, and Mingsheng Long. Non-stationary transformers: Exploring the stationarity in time series forecasting. *Advances in Neural Information Processing Systems*, 35:9881–9893, 2022b.

Yong Liu, Tengge Hu, Haoran Zhang, Haixu Wu, Shiyu Wang, Lintao Ma, and Mingsheng Long. itransformer: Inverted transformers are effective for time series forecasting. *arXiv preprint arXiv:2310.06625*, 2023.

Donghao Luo and Xue Wang. Moderntcn: A modern pure convolution structure for general time series analysis. In *The Twelfth International Conference on Learning Representations*, 2024.

Xiang Ma, Xuemei Li, Lexin Fang, Tianlong Zhao, and Caiming Zhang. U-mixer: An unet-mixer architecture with stationarity correction for time series forecasting. In *Proceedings of the AAAI Conference on Artificial Intelligence*, volume 38, pp. 14255–14262, 2024.

Spyros Makridakis, Evangelos Spiliotis, and Vassilios Assimakopoulos. The m4 competition: Results, findings, conclusion and way forward. *International Journal of forecasting*, 34(4):802–808, 2018.

Aditya P Mathur and Nils Ole Tippenhauer. Swat: A water treatment testbed for research and training on ics security. In *2016 international workshop on cyber-physical systems for smart water networks (CySWater)*, pp. 31–36. IEEE, 2016.

Yue Meng, Rameswar Panda, Chung-Ching Lin, Prasanna Sattigeri, Leonid Karlinsky, Kate Saenko, Aude Oliva, and Rogerio Feris. Adafuse: Adaptive temporal fusion network for efficient action recognition. *arXiv preprint arXiv:2102.05775*, 2021.

Yuqi Nie, Nam H Nguyen, Phanwadee Sinthong, and Jayant Kalagnanam. A time series is worth 64 words: Long-term forecasting with transformers. *arXiv preprint arXiv:2211.14730*, 2022.

Zijie Pan, Yushan Jiang, Sahil Garg, Anderson Schneider, Yuriy Nevmyvaka, and Dongjin Song. S2ip-llm: Semantic space informed prompt learning with llm for time series forecasting. In *Forty-first International Conference on Machine Learning*, 2024.

Guansong Pang, Chunhua Shen, Longbing Cao, and Anton Van Den Hengel. Deep learning for anomaly detection: A review. *ACM computing surveys (CSUR)*, 54(2):1–38, 2021.

Adam Paszke, Sam Gross, Francisco Massa, Adam Lerer, James Bradbury, Gregory Chanan, Trevor Killeen, Zeming Lin, Natalia Gimelshein, Luca Antiga, et al. Pytorch: An imperative style, high-performance deep learning library. *Advances in neural information processing systems*, 32, 2019.

Ya Su, Youjian Zhao, Chenhao Niu, Rong Liu, Wei Sun, and Dan Pei. Robust anomaly detection for multivariate time series through stochastic recurrent neural network. In *Proceedings of the 25th ACM SIGKDD international conference on knowledge discovery & data mining*, pp. 2828–2837, 2019.

Ao Wang, Hui Chen, Zijia Lin, Jungong Han, and Guiguang Ding. Repvit: Revisiting mobile cnn from vit perspective. In *Proceedings of the IEEE/CVF Conference on Computer Vision and Pattern Recognition*, pp. 15909–15920, 2024a.

Huiqiang Wang, Jian Peng, Feihu Huang, Jince Wang, Junhui Chen, and Yifei Xiao. Micn: Multi-scale local and global context modeling for long-term series forecasting. In *The eleventh international conference on learning representations*, 2023.

Yuxuan Wang, Haixu Wu, Jiaxiang Dong, Yong Liu, Yunzhong Qiu, Haoran Zhang, Jianmin Wang, and Mingsheng Long. Timexer: Empowering transformers for time series forecasting with exogenous variables. *arXiv preprint arXiv:2402.19072*, 2024b.

Haixu Wu, Jiehui Xu, Jianmin Wang, and Mingsheng Long. Autoformer: Decomposition transformers with auto-correlation for long-term series forecasting. *Advances in neural information processing systems*, 34:22419–22430, 2021.

Haixu Wu, Tengge Hu, Yong Liu, Hang Zhou, Jianmin Wang, and Mingsheng Long. Timesnet: Temporal 2d-variation modeling for general time series analysis. *arXiv preprint arXiv:2210.02186*, 2022a.

Haixu Wu, Jialong Wu, Jiehui Xu, Jianmin Wang, and Mingsheng Long. Flowformer: Linearizing transformers with conservation flows. *arXiv preprint arXiv:2202.06258*, 2022b.

Jiehui Xu, Haixu Wu, Jianmin Wang, and Mingsheng Long. Anomaly transformer: Time series anomaly detection with association discrepancy. *arXiv preprint arXiv:2110.02642*, 2021.

Brandon Yang, Gabriel Bender, Quoc V Le, and Jiquan Ngiam. Condconv: Conditionally parameterized convolutions for efficient inference. *Advances in neural information processing systems*, 32, 2019.

Ailing Zeng, Muxi Chen, Lei Zhang, and Qiang Xu. Are transformers effective for time series forecasting? In *Proceedings of the AAAI conference on artificial intelligence*, volume 37, pp. 11121–11128, 2023.

Tianping Zhang, Yizhuo Zhang, Wei Cao, Jiang Bian, Xiaohan Yi, Shun Zheng, and Jian Li. Less is more: Fast multivariate time series forecasting with light sampling-oriented mlp structures. *arXiv preprint arXiv:2207.01186*, 2022.

Yao Zhang, Jianxue Wang, and Xifan Wang. Review on probabilistic forecasting of wind power generation. *Renewable and Sustainable Energy Reviews*, 32:255–270, 2014.

Yunhao Zhang and Junchi Yan. Crossformer: Transformer utilizing cross-dimension dependency for multivariate time series forecasting. In *The eleventh international conference on learning representations*, 2023.

Haoyi Zhou, Shanghang Zhang, Jieqi Peng, Shuai Zhang, Jianxin Li, Hui Xiong, and Wancai Zhang. Informer: Beyond efficient transformer for long sequence time-series forecasting. In *Proceedings of the AAAI conference on artificial intelligence*, volume 35, pp. 11106–11115, 2021.

Tian Zhou, Ziqing Ma, Qingsong Wen, Xue Wang, Liang Sun, and Rong Jin. Fedformer: Frequency enhanced decomposed transformer for long-term series forecasting. In *International conference on machine learning*, pp. 27268–27286. PMLR, 2022.

A TVNet theoretical discussions

Problem Definition: (Time Series Analysis) Time series analysis encompasses five primary subtasks: long-term forecasting, short-term forecasting, interpolation, classification, and anomaly detection. Mathematically, these tasks are defined with respect to a look back window $X \in \mathbb{R}^{L \times C}$, where L is the window length and C is the number of features. The goal is to develop a deep-learning model f that minimizes the prediction error $e(Y, f(X))$. The target output Y varies by task: - For forecasting: $Y \in \mathbb{R}^{T1 \times C_o}$, where $T1$ is the forecast horizon and C_o is the number of output features. - For imputation and anomaly detection: $Y \in \mathbb{R}^{T2 \times C_o}$, where $T2$ is the data length for imputation or anomaly detection and C_o is the number of output features. - For classification: $Y \in \mathbb{R}^{1 \times C}$, where C represents the number of classification labels.

Algorithm 2 3D-Embedding applied to general time series analysis.

```
Require: Look back window $X \in \mathbb{R}^{L \times C}$, where $L$ is the length of the time series and $C$ is the number of channels.
Embed the input along the feature dimensions $C$ to get $X' \in \mathbb{R}^{L \times C_m}$, where $C_m$ is the embedding dimension.
Use Conv1D (kernel size = $P$) to divide $X'$ into $N$ patches $x_i \in \mathbb{R}^{P \times C_m}$, where $N = \frac{L}{P}$.
for $i = 1$ to $N$ do
    Split each patch $x_i$ by odd and even indices to get $x_{odd}, x_{even} \in \mathbb{R}^{P/2 \times C_m}$.
    Concatenate $x_{odd}$ and $x_{even}$ to get $x_i \in \mathbb{R}^{2 \times (P/2) \times C_m}$.
end for
Concatenate all patches to get $X_{emb} \in \mathbb{R}^{N \times 2 \times (P/2) \times C_m}$.
```

A.1 Theoretical Analysis

Theorem B.1: Under appropriate optimization, the dynamic weight model achieves a lower error than the fixed weight model, i.e., $E_d < E_f$.

Definition: In the context of time series analysis, we can segment a dataset into N distinct patches, denoted as $x_1, x_2, \ldots, x_N$, each with its corresponding true target value y_i^*. Two models are considered for processing these patches:

Fixed Weight Model: This model employs a constant weight W_f to produce the convolution output for each patch i. The output is calculated as follows:

$$y_{f,i} = W_f \cdot x_i \tag{10}$$

This model uses variable weights W_i for each patch, defined as $W_i = \alpha_i \cdot W_b$, where α_i is a coefficient that can vary with each patch. The convolution output for patch i is then given by:

$$y_{d,i} = W_i \cdot x_i = (\alpha_i \cdot W_b) \cdot x_i \tag{11}$$

Proof:

For the fixed weight model, the total error is given by:

$$E_f = \sum_{i=1}^{N} (W_f \cdot x_i - y_i^*)^2 \tag{12}$$

Expanding the square term, we get:

$$E_f = \sum_{i=1}^{N} \left((W_f \cdot x_i)^2 - 2W_f \cdot x_i \cdot y_i^* + (y_i^*)^2 \right) \tag{13}$$

For the dynamic weight model, the total error is given by:

$$E_d = \sum_{i=1}^{N} ((\alpha_i \cdot W_b \cdot x_i) - y_i^*)^2 \tag{14}$$

Expanding the square term, we get:

$$E_d = \sum_{i=1}^{N} \left((\alpha_i \cdot W_b \cdot x_i)^2 - 2(\alpha_i \cdot W_b \cdot x_i) \cdot y_i^* + (y_i^*)^2 \right) \tag{15}$$

In the fixed weight model, the error E_f is minimized by optimizing the single parameter W_f:

$$\frac{\partial E_f}{\partial W_f} = 0 \quad \Rightarrow \quad W_f = \text{optimal fixed weight} \tag{16}$$

In the dynamic weight model, the error E_d is minimized by optimizing both W_b (shared across patches) and α_i (specific to each patch). The optimization conditions are:

$$\frac{\partial E_d}{\partial W_b} = 0 \quad \text{and} \quad \frac{\partial E_d}{\partial \alpha_i} = 0, \forall i \tag{17}$$

Solving for α_i:

$$\alpha_i = \frac{y_i^*}{W_b \cdot x_i}, \forall i \tag{18}$$

Substituting this back into E_d, the error is further reduced compared to the fixed weight model.

The dynamic weight model provides additional flexibility by adjusting α_i for each patch i. This allows it to better approximate the target y_i^*, resulting in:

$$E_d < E_f \tag{19}$$

A.2 Computational Analysis:

Consider the input time series tensor $X^{3D} \in \mathbb{R}^{C_m \times N \times 2 \times \frac{P}{2}}$, where $N \times P = L$ and L represents the time series length. Given that the output dimension of TVNet matches the input dimensions, the computational complexity for 2D convolutions can be described as follows:

$$\begin{aligned} \text{FLOPs(Conv2D)} = C_m \times C_m \times k^2 \times N \times 2 \times (P/2) = C_m \times C_m \times k^2 \times L \\ \text{Params(Conv2d)} = C_m \times C_m \times k^2 \end{aligned} \tag{20}$$

C_m denote the embedding dimensions and k represent the kernel size of the 2D convolutions. In the process of generating time-varying weights, the features are initially passed through an intra-pool and subsequently through an inter-pool, which incorporates a non-parameter layer.

$$\begin{aligned} \text{FLOPs}(\mathcal{G}_{intra}) = C_m \times N \times 2 \times P/2 = C_m \times L \\ \text{Params}(\mathcal{G}_{inter}) = C_m \times N \end{aligned} \tag{21}$$

In the channel modeling process, two 1D convolutions with a kernel size of $k = 1$ are utilized.

$$\begin{aligned} \text{FLOPs(channel)} = C_m \times C_m \times k(1) \times N + C_m \times C_m \times k(1) \\ \text{Params(channel)} = C_m \times C_m \times k(1) + C_m \times C_m \times k(1) \end{aligned} \tag{22}$$

Subsequently, the time-varying weight matrix $\alpha \in \mathbb{R}^{C_m \times N}$ is multiplied by the temporal weight tensor $W \in \mathbb{R}^{C_m \times C_m \times k^2}$ for 2D convolutions.

$$\text{FLOPs(multipy)} = C_m \times C_m \times k^2 \times N \tag{23}$$

Therefore, the total computational complexity and parameter count are as follows:

$$\begin{aligned} \text{FLOPs} =& \text{FLOPs(Conv2D)} + \text{FLOPs}(\mathcal{G}) + \text{FLOPs(channel)} + \text{FLOPs(multiply)} \\ &= C_m \times L + C_m \times L + C_m \times C_m \times k(1) \times N \\ &+ C_m \times C_m \times k(1) + C_m \times C_m \times k^2 \times N \end{aligned} \tag{24}$$

$$\begin{aligned} \text{Params} =& \text{Params(Conv2D)} + \text{Params}(\mathcal{G}) + \text{Params(channel)} \\ &= C_m \times C_m \times k^2 + C_m \times N + C_m \times C_m \times k(1) + C_m \times C_m \times k(1) \end{aligned} \tag{25}$$

Based on the computational analysis, TVNet demonstrates FLOPs of $O(LC_m^2)$ and a parameter count of $O(C_m^2)$.

B DATASETS

B.1 LONG-TERM FORECAST AND IMPUTATION DATASETS

Assessments of the long-term forecasting capabilities were conducted using nine widely recognized real-world datasets, encompassing domains such as weather, traffic, electricity, exchange rates, influenza-like illness (ILI), and the four Electricity Transformer Temperature (ETT) datasets (ETTh1, ETTh2, ETTm1, ETTm2). For the imputation task, benchmarks were established using datasets from weather, electricity, and the four ETT datasets. These datasets, extensively utilized in the field, cover various aspects of daily life.

The characteristics of each dataset, including the total number of timesteps, the count of variables, and the sampling frequency, are summarized in Table 7. The datasets are partitioned into training, validation, and testing subsets in chronological order, with the Electricity Transformer Temperature (ETT) dataset employing a 6:2:2 ratio and the remaining datasets using a 7:1:2 ratio. Normalization to a zero mean is applied to the training, validation, and testing subsets based on the mean and standard deviation of the training subset. Each dataset comprises a single, continuous, long-time series, with samples extracted using a sliding window technique.

Further details regarding the datasets are as follows:

1. ***Weather***[1] consists of 21 climatic variables, such as humidity and air temperature, recorded in Germany throughout 2020.
2. ***Traffic***[2] includes road occupancy rates collected by 862 sensors across San Francisco Bay area highways over a two-year period, provided by the California Department of Transportation.
3. ***Electricity***[3] comprises hourly electricity usage data for 321 consumers from 2012 to 2014.
4. ***Exchange***[4] encompasses daily exchange rates for eight currencies, observed from 1990 to 2016.
5. ***ILI***[5], which stands for Influenza-Like Illness, contains weekly counts of ILI patients in the United States from 2002 to 2021. It includes seven metrics, such as ILI patient counts across various age groups and the proportion of ILI patients relative to the total patient population. The data is provided by the Centers for Disease Control and Prevention of the United States.
6. ***ETT***[6], The Electricity Transformer Temperature (ETT) dataset comprises data from seven sensors across two Chinese counties, featuring load and oil temperature metrics. It includes four subsets: 'ETTh1' and 'ETTh2' for hourly data, and 'ETTm1' and 'ETTm2' for 15-minute intervals.

Table 7: Dataset descriptions of long-term forecasting and imputation.

Dataset	Weather	Traffic	Exchange	Electricity	ILI	ETTh1	ETTh2	ETTm1	ETTm2
Dataset Size	52696	17544	7207	26304	966	17420	17420	69680	69680
Variable Number	21	862	8	321	7	7	7	7	7
Sampling Frequency	10 mins	1 hour	1 day	1 hour	1 week	1 hour	1 hour	15 mins	15 mins

B.2 SHORT-TERM FORECAST DATASETS

The M4 dataset, which includes 100,000 heterogeneous time series from various domains, poses a unique challenge for short-term forecasting. This is attributed to the diverse origins and distinct

[1] https://www.bgc-jena.mpg.de/wetter/

[2] https://pems.dot.ca.gov/

[3] https://archive.ics.uci.edu/dataset/321/electricityloaddiagrams20112014

[4] https://github.com/laiguokun/multivariate-time-series-data

[5] https://github.com/laiguokun/multivariate-time-series-data

[6] https://github.com/zhouhaoyi/ETDataset

temporal characteristics of the data, which contrast with the uniformity typically found in long-term forecasting datasets. A statistical overview of the dataset is provided in Table 8.

Table 8: Dataset descriptions of M4 forecasting

Dataset	Sample Numbers (train set, test set)	Variable Number	Prediction Length
M4 Yearly	(23000, 23000)	1	6
M4 Quarterly	(24000, 24000)	1	8
M4 Monthly	(48000, 48000)	1	18
M4 Weekly	(359, 359)	1	13
M4 Daily	(4227, 4227)	1	14
M4 Hourly	(414, 414)	1	48

B.3 Classification datasets

The UEA dataset comprises a diverse collection of time series samples across various domains, designed for classification tasks. It encompasses a broad spectrum of recognition tasks, including facial, gesture, and action recognition, as well as audio identification. Furthermore, it extends its utility to practical applications in industrial monitoring, health surveillance, and medical diagnostics, with a particular emphasis on the analysis of cardiac data. Typically, the dataset is organized into 10 distinct classes. Table 9 offers a detailed overview of the classification statistics for the UEA datasets, underscoring their extensive applicability across multiple domains.

Table 9: Datasets and mapping details of UEA dataset

Dataset	Sample Numbers (train set, test set)	Variable Number	Series Length
EthanolConcentration	(261, 263)	3	1751
FaceDetection	(5890, 3524)	144	62
Handwriting	(150, 850)	3	152
Heartbeat	(204, 205)	61	405
JapaneseVowels	(270, 370)	12	29
PEMS - SF	(267, 173)	963	144
SelfRegulationSCP1	(268, 293)	6	896
SelfRegulationSCP2	(200, 180)	7	1152
SpokenArabicDigits	(6599, 2199)	13	93
UWaveGestureLibrary	(120, 320)	3	315

B.4 Anomaly detection datasets

Our benchmarking process utilizes datasets that cover a range of domains, such as server machinery, spacecraft, and infrastructure systems. These datasets are carefully organized into three distinct phases: training, validation, and testing. Each dataset consists of a single, continuous time series, and samples are extracted using a uniform, fixed-length sliding window method. Table 10 presents a comprehensive statistical summary of these datasets, illustrating their structured arrangement and the systematic approach to sample extraction.

Table 10: Dataset sizes and details for anomaly detection datasets

Dataset	Dataset sizes (train set, val set, test set)	Variable Number	Sliding Window Length
SMD	(566724, 141681, 708420)	38	100
MSL	(44653, 11664, 73729)	55	100
SMAP	(108146, 27037, 427617)	25	100
SWaT	(396000, 99000, 449919)	51	100
PSM	(105984, 26497, 87841)	25	100

B.5 DATASET VISUALIZATION

Figure 9,10,11 and 12 shows the pairwise correlation among the variables in ETT dataset.

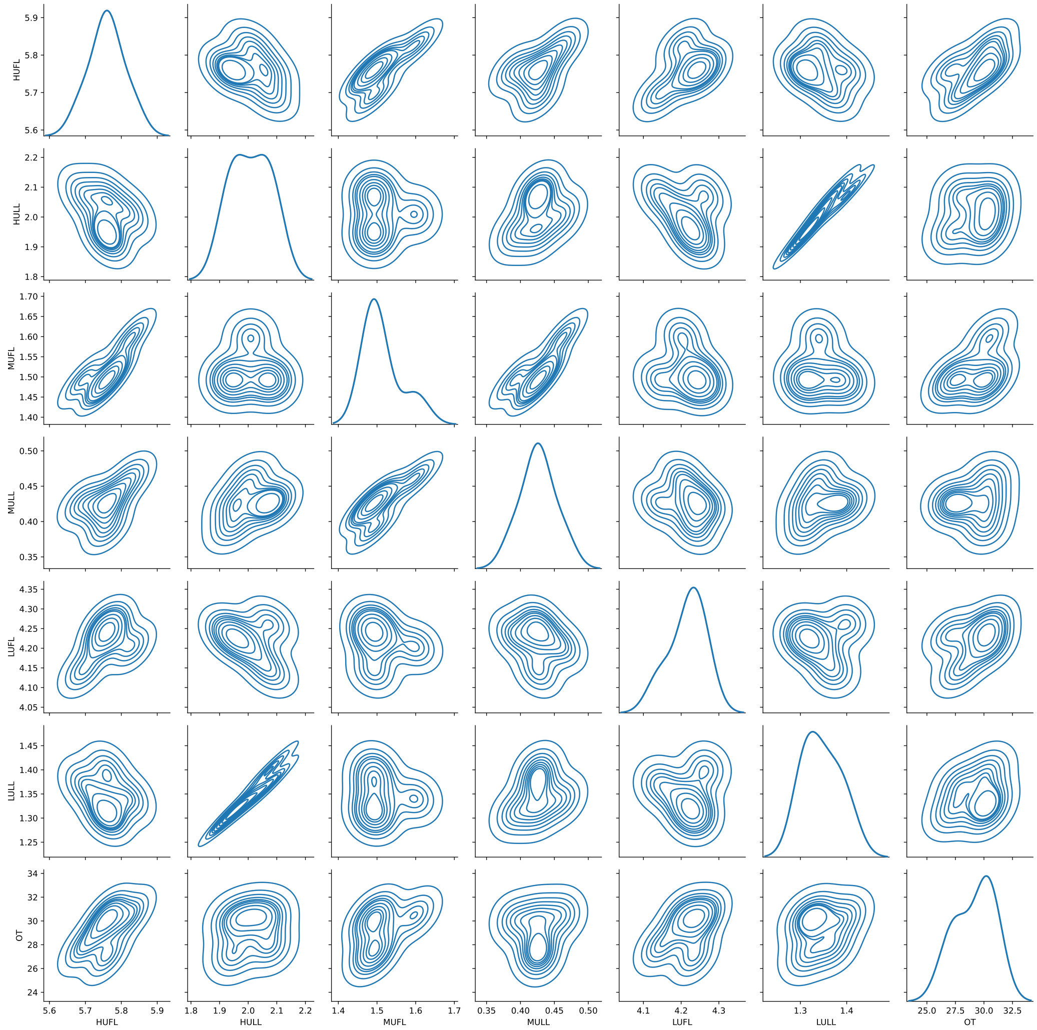

Figure 9: Pairwise correlation among the variables(ETTm1).

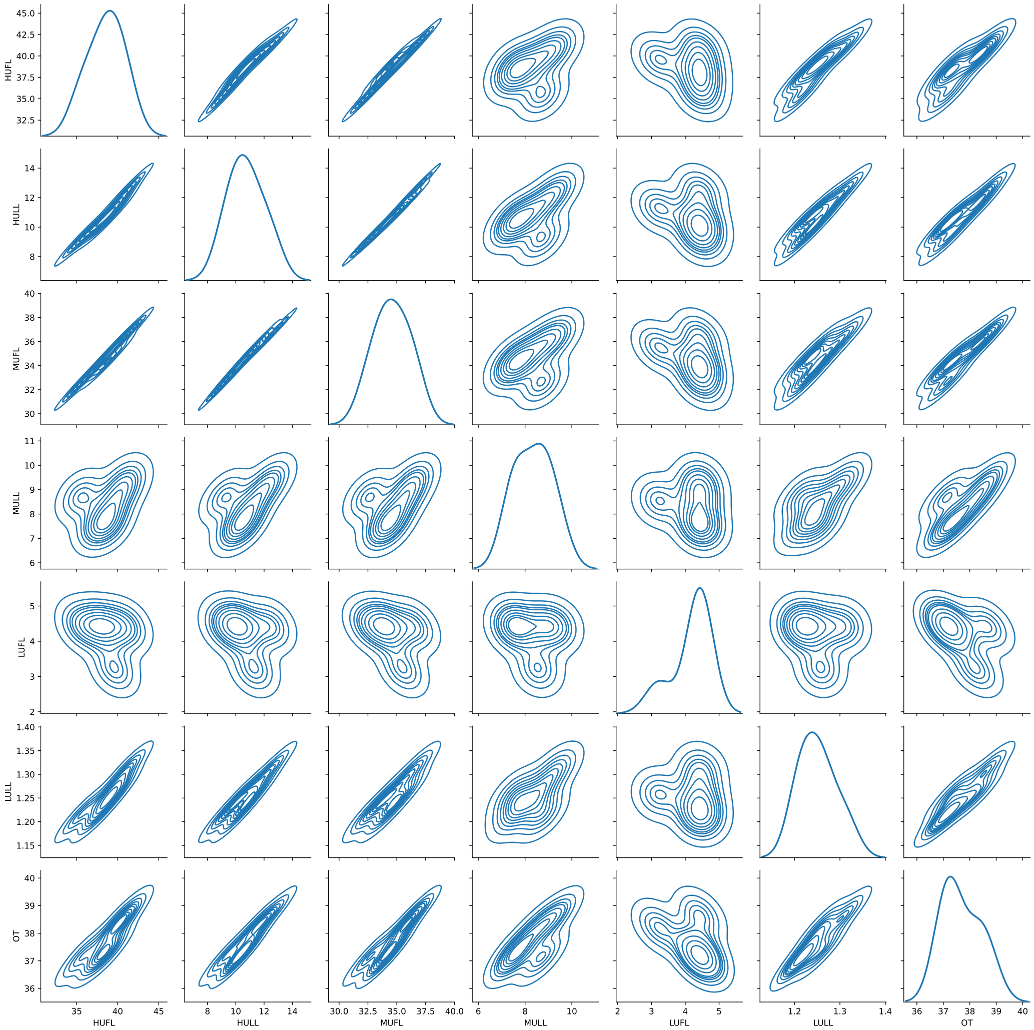

Figure 10: Pairwise correlation among the variables(ETTm2).

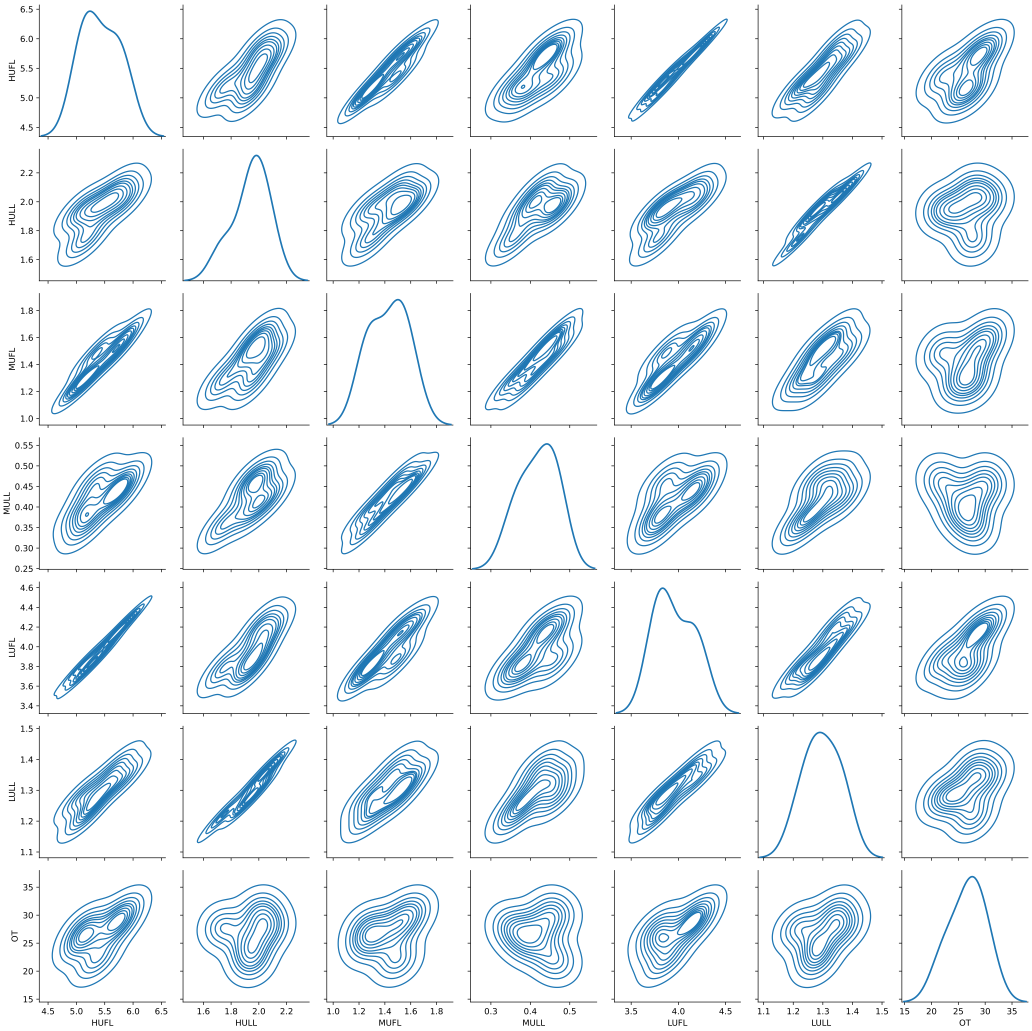

Figure 11: Pairwise correlation among the variables(ETTh1).

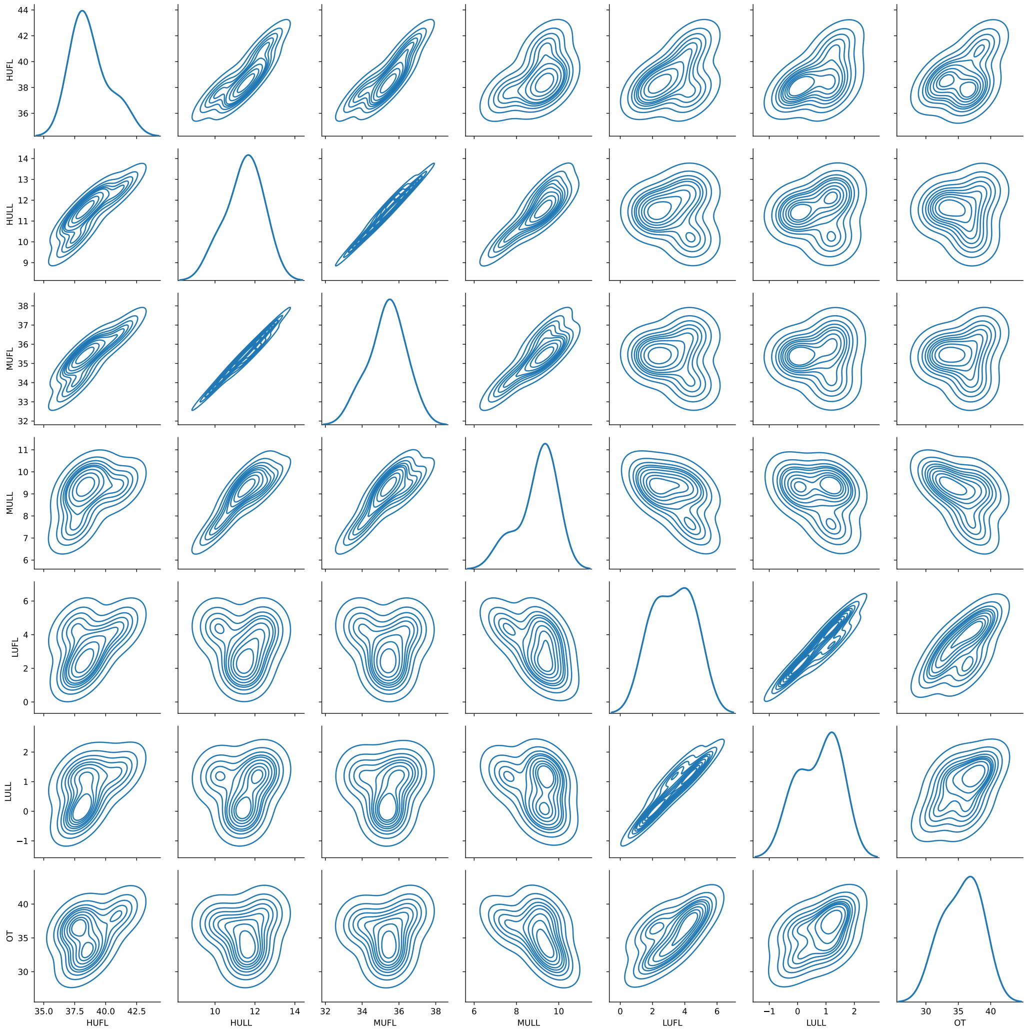

Figure 12: Pairwise correlation among the variables(ETTh2).

C Experiment details

Table 11: Model Hyper-parameters and Training Process for Different Tasks/Configurations(TVNet)

Tasks/Configurations	Model Hyper-parameter				Training Process			
	k (kernel size)	Layers	C_m	P (Patch length)	LR	Loss	Batch Size	Epochs
Long-term Forecasting	$3x3$	3	64	24	10^{-4}	MSE	32	10
Short-term Forecasting	$3x3$	3	64	8	10^{-3}	SMAPE	16	10
Imputation	$3x3$	3	64	1	10^{-3}	MSE	16	10
Classification	$3x3$	3	Eq31	1	10^{-3}	Cross Entropy	16	30
Anomaly Detection	$3x3$	5	Eq32	8	10^{-4}	MSE	128	10

- LR refers to the learning rate, and we have incorporated an early stopping mechanism to enhance the training process.For long-term forecasting task,Input lenght is set to 96Wu et al. (2022a).
- We performed experiments using 5 distinct random seeds: 1111, 333, 2023, 2024, and 2025.

C.1 Long-term forecasting

Implementation details: Our method utilizes the mean squared error (MSE) loss function and is optimized using the ADAM optimizer (Kingma, 2014), with an initial learning rate set to 10^{-4}. The training regimen consists of 10 epochs, augmented by an appropriate early stopping mechanism. We employ the mean squared error (MSE) and mean absolute error (MAE) as evaluation metrics. The deep learning models are implemented using PyTorch (Paszke et al., 2019) and executed on NVIDIA RTX4090 GPU.

Model parameter: TVNet comprises 3 3D-blocks, with the embedding dimensions (C_m) set to 64. The patch length (P) is established at 24, and the kernel size (k) for 2D convolutions is 3×3. The random seed is set to 2024.

Metrics: The mean square error (MSE) and mean absolute error (MAE) are adopted for long-term forecasting.

$$MSE = \frac{1}{T}\sum_{i=0}^{T}(\widehat{x}_i - x_i)^2 \tag{26}$$

$$MAE = \frac{1}{T}\sum_{i=0}^{T}|\widehat{x}_i - x_i| \tag{27}$$

where T is the number of observations, $\widehat{x}_i$ is the predicted value, and x_i is the actual value for observation i.

C.2 Short-term forecasting

Implementation details: Our method employs the Symmetric Mean Absolute Percentage Error (SMAPE) loss function and is optimized using the ADAM optimizer (Kingma, 2014), with an initial learning rate of 10^{-3}. The training regimen consists of 10 epochs, augmented by an appropriate early stopping mechanism. We utilize the SMAPE, Mean Absolute Scaled Error (MASE), and Overall Weighted Average (OWA) as evaluation metrics.

Model parameter: TVNet consists of 3 3D-blocks, with the embedding dimension C_m configured to 64. The patch length P is set to 8, and the kernel size k for 2D convolutions is 3×3.The random seed is set to 2024.

Metrics: For short-term forecasting, in accordance with (Wu et al., 2022a), we utilize the Symmetric Mean Absolute Percentage Error (SMAPE), Mean Absolute Scaled Error (MASE), and Overall Weighted Average (OWA) as the metrics. These metrics can be computed as follows:

$$\text{SMAPE} = \frac{200}{T}\sum_{i=1}^{T}\frac{|x_i - \widehat{x}_i|}{|x_i| + |\widehat{x}_i|} \tag{28}$$

$$\text{MASE} = \frac{1}{T}\sum_{i=1}^{T}\frac{|x_i - \widehat{x}_i|}{\frac{1}{T-p}\sum_{j=p+1}^{T}|x_j - x_{j-p}|} \tag{29}$$

$$\text{OWA} = \frac{1}{2}\left[\frac{\text{SMAPE}}{\text{SMAPE}_{\text{Naive2}}} + \frac{\text{MASE}}{\text{MASE}_{\text{Naive2}}}\right] \tag{30}$$

where p is the periodicity of data, T is the number of observations, $\widehat{x}_i$ is the predicted value, and x_i is the actual value for observation i.

C.3 Imputation

Implementation details: Our method utilizes the mean squared error (MSE) loss function and is optimized using the ADAM optimizer (Kingma, 2014), with an initial learning rate set to 10^{-3}. The training regimen consists of 10 epochs, augmented by an appropriate early stopping mechanism. We employ the mean squared error (MSE) and mean absolute error (MAE) as evaluation metrics.

Model parameter: TVNet has 3 blocks.The patch length P is set to 1 to avoid mixing the masked and unmasked tokens, with the embedding dimension C_m configured to 64.The random seed is set to 2024

C.4 Classification

Implementation details: Our method employs the Cross-Entropy Loss and is optimized using the ADAM optimizer, initialized with a learning rate of 10^{-3}. The training regimen consists of 30 epochs, complemented by an appropriate early stopping mechanism. Classification accuracy serves as the metric for evaluation.

Model parameter: By default, TVNet comprises 3 blocks. The equation determines the channel number C_m.The random seed is set to 2024.

$$C_m = \min\left\{\max\left(2^{\lfloor \log_2 M \rfloor}, d_{\min}\right), d_{\max}\right\} \tag{31}$$

where $d_{\min}$ is 32 and $d_{\max}$ is 64, in accordance with the predefined criteria. The patch length P is established at 1.

Metrics: For classification, the accuracy is calculated as the metric.

C.5 Anomaly detection

Implementation details: In the classical reconstruction task, we employ MSE loss for training. The ADAM optimizer is utilized, initialized with a learning rate of $\times 10^{-4}$. The training regimen consists of 10 epochs, complemented by an appropriate early stopping mechanism. The reconstruction error, quantified as the Mean Squared Error (MSE), serves as the criterion for anomaly detection. The F1-Score is adopted as the metric.

Model parameter: By default, TVNet comprises 3 blocks. The channel number C_m is determined by the equation

$$C_m = \min\left\{\max\left(2^{\lfloor \log_2 M \rfloor}, d_{\min}\right), d_{\max}\right\} \tag{32}$$

where $d_{\min}$ is 32 and $d_{\max}$ is 128, in accordance with the predefined criteria. The patch length P is established at 8.

Metrics: For anomaly detection, we adopt the F1-score, which is the harmonic mean of precision and recall.

D Hyperparameter sensitivity

D.1 Model Hyperparameters

In this section, we assess the robustness of TVNet by examining its sensitivity to model hyperparameters. We will meticulously assess the impact of hyperparameter tuning on long-term forecasting models, focusing on the embedding dimensions(C_m), the number of blocks, and the patch length(P) and kernel size(k) to enhance the accuracy of our predictions.

Embedding Dimensions and Number of blocks:Figure 13 shows the different effect about DataEmbedding dimension($C_m = 32, 64, 128, 512$) and the number of 3D-blocks($1, 2, 3, 4, 5$) on ETT datasets(Prediction length = 96).Table 12 shows the effects of different $C_m$on the three data sets(ETTh1,Weather and Electricity) for long-term prediction tasks of different prediction lengths.For Cm, with the increase of dimension, MSE and MAE show an upward trend on ETTh1 and Weather datasets, but decrease first and then increase on Electricity datasets. In general, we can see that for different C_m, although the value of forecasting varies over the long term, the overall volatility is small.

We tested the influence of different 3D-Blocks(L) on task prediction results in long-term forecasting,short-term forecasting and Anomaly detection.(Table 13,Table 14,Table 15) For long-term forecasting and short-term forecasting, $L = 2, 3, 4$ is tested; for Anomaly detection, $L = 4, 5, 6$ is tested. The selection of $L$is based on Table 11. The results show that as the number of 3D-block layers increases, the accuracy of prediction and anomaly detection generally increases slightly, which indicates that a single 3D-block has good time series characterization ability without relying on deep stacking. According to the above results, the model shows better robustness for DataEmbedding Dimension $C_m$and the number of 3D-Blocks.

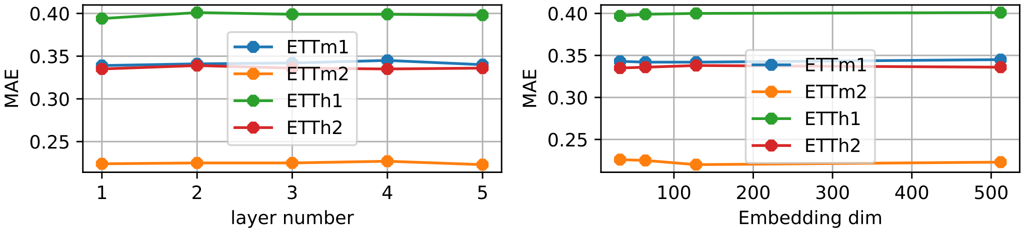

Figure 13: Hyperparameter sensitivity concerning the dimension of DataEmbedding and number of blocks

Table 12: Impact of different DataEmbedding dimension. A lower MSE or MAE indicates a better performance.

Models	Metrics	ETTh1				Weather				Electricity			
		96	192	336	720	96	192	336	720	96	192	336	720
$C_m = 32$	MSE	0.369	0.399	0.403	0.460	0.149	0.192	0.235	0.306	0.139	0.168	0.162	0.189
	MAE	0.407	0.409	0.414	0.457	0.195	0.237	0.281	0.336	0.228	0.246	0.265	0.287
$C_m = 64$	MSE	0.371	0.398	0.401	0.458	0.147	0.194	0.235	0.308	0.142	0.165	0.164	0.190
	MAE	0.408	0.409	0.409	0.459	0.198	0.238	0.277	0.331	0.223	0.241	0.269	0.284
$C_m = 128$	MSE	0.365	0.389	0.395	0.451	0.153	0.187	0.240	0.306	0.140	0.157	0.166	0.182
	MAE	0.404	0.403	0.406	0.453	0.196	0.235	0.276	0.329	0.219	0.238	0.270	0.285

Table 13: Impact of different number of 3D-Blocks(L). A lower MSE or MAE indicates a better performance.

Models	Metrics	ETTh1				Weather				Electricity			
		96	192	336	720	96	192	336	720	96	192	336	720
$L = 2$	MSE	0.380	0.412	0.413	0.479	0.153	0.199	0.242	0.316	0.146	0.169	0.168	0.197
	MAE	0.410	0.419	0.417	0.475	0.202	0.244	0.285	0.339	0.230	0.247	0.275	0.291
$L = 3$	MSE	0.371	0.398	0.401	0.458	0.147	0.194	0.235	0.308	0.142	0.165	0.164	0.190
	MAE	0.408	0.409	0.409	0.459	0.198	0.238	0.277	0.331	0.223	0.241	0.269	0.284
$L = 4$	MSE	0.360	0.382	0.387	0.435	0.143	0.190	0.229	0.299	0.139	0.161	0.159	0.185
	MAE	0.399	0.402	0.399	0.443	0.194	0.232	0.275	0.321	0.216	0.235	0.269	0.277

Table 14: Impact of different number of 3D-Blocks(L) for short-term forecasting

Models	Yearly			Quarterly			Monthly			Others		
	SMAPE	MASE	OWA	SMAEP	MASE	OWA	SMAPE	MASE	OWA	SMAPE	MASE	OWA
$L = 2$	13.596	3.124	0.826	10.941	1.305	1.064	12.729	0.951	0.885	4.951	3.121	1.035
$L = 3$	13.217	2.899	0.768	9.986	1.159	0.876	12.493	0.921	0.866	4.764	2.986	0.969
$L = 4$	13.199	2.871	0.754	9.981	1.152	0.876	12.490	0.923	0.867	4.752	2.981	0.965

Table 15: Impact of different number of 3D-Blocks(L) for Anomaly detection(F1)

Dataset	Model	SMD	MSL	SMAP	SWaT	PSM
$L = 4$	Ours	84.93	85.10	71.21	93.54	97.45
$L = 5$	Ours	85.75	85.16	71.64	93.72	97.53
$L = 6$	Ours	85.79	85.20	71.59	93.81	97.67

Patch length and Kernel size: In this section, we conducted experiments on long-term forecasting tasks by varying the Patch length (P) and Kernel size (k). We tested four distinct values for Patch length $(8, 12, 24, 32)$ on long-term forecasting.Further, we test different Patch lengths (P) in long-term forecasting and short-term forecasting(Table 17,Table 16), and the results show that TVNet is robust when a moderate Patch length is selected. Different P has no significant influence on the result.To maintain the dimensionality of each feature map layer, we employed zero-padding equivalent to `(kernel size - 1)`. The results presented in Table 18 indicate that both extremely small and large convolution kernels negatively impact the prediction accuracy. This study advocates for the adoption of a 3×3 convolution kernel, which strikes a balance between capturing local features and maintaining computational efficiency.For the Patch length (P), our findings indicate that both smaller and larger values can degrade the forecasting performance. In the context of long-term forecasting, we recommend setting the Patch length to 24, as it offers an optimal balance for prediction accuracy. For short term forecasting, 8 is recommended for patch-length.

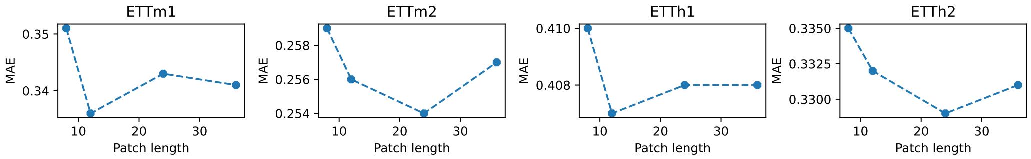

Figure 14: Hyperparameter sensitivity concerning patch length(prediction length=96)

Table 16: Impact of different Patch length.A lower MSE or MAE indicates a better performance.

Models	Metrics	ETTh1				Weather				Electricity			
		96	192	336	720	96	192	336	720	96	192	336	720
$P = 8$	MSE	0.384	0.406	0.404	0.463	0.153	0.197	0.236	0.309	0.147	0.163	0.172	0.193
	MAE	0.413	0.417	0.412	0.463	0.204	0.251	0.286	0.334	0.226	0.247	0.272	0.289
$P = 12$	MSE	0.369	0.404	0.402	0.449	0.153	0.205	0.237	0.311	0.146	0.170	0.163	0.191
	MAE	0.406	0.411	0.412	0.463	0.209	0.245	0.287	0.332	0.227	0.246	0.265	0.280
$P = 24$	MSE	0.371	0.398	0.401	0.458	0.147	0.194	0.235	0.308	0.142	0.165	0.164	0.190
	MAE	0.408	0.409	0.409	0.459	0.198	0.238	0.277	0.331	0.223	0.241	0.269	0.284
$P = 32$	MSE	0.368	0.395	0.399	0.454	0.150	0.192	0.241	0.311	0.145	0.167	0.155	0.192
	MAE	0.401	0.407	0.420	0.457	0.205	0.239	0.277	0.332	0.227	0.242	0.252	0.288

Table 17: Impact of different Patch length(P) for short-term forecasting

Models	Metrics	Yearly			Quarterly			Monthly			Others		
		SMAPE	MASE	OWA	SMAEP	MASE	OWA	SMAPE	MASE	OWA	SMAPE	MASE	OWA
$P = 4$		13.151	2.925	0.765	10.056	1.155	0.885	12.382	0.926	0.859	4.792	2.965	0.977
$P = 8$		13.217	2.899	0.768	9.986	1.159	0.876	12.493	0.921	0.866	4.764	2.986	0.969
$P = 16$		13.073	2.871	0.754	9.903	1.147	0.873	12.348	0.912	0.854	4.664	2.977	0.955

Table 18: Impact of different kernel sizes. A lower MSE or MAE indicates a better performance.

Models	Metrics	ETTh1				ETTm1				Electricity			
		96	192	336	720	96	192	336	720	96	192	336	720
$k = 1$	MSE	0.375	0.407	0.405	0.464	0.293	0.327	0.371	0.412	0.143	0.171	0.169	0.196
	MAE	0.413	0.417	0.415	0.464	0.358	0.371	0.392	0.419	0.221	0.249	0.265	0.302
$k = 3$	MSE	0.371	0.398	0.401	0.458	0.288	0.326	0.365	0.412	0.142	0.165	0.164	0.190
	MAE	0.408	0.409	0.409	0.459	0.343	0.367	0.391	0.413	0.223	0.241	0.269	0.284
$k = 5$	MSE	0.369	0.396	0.399	0.454	0.289	0.324	0.367	0.417	0.146	0.168	0.165	0.187
	MAE	0.405	0.408	0.409	0.457	0.339	0.362	0.390	0.415	0.220	0.240	0.264	0.279
$k = 7$	MSE	0.370	0.399	0.398	0.450	0.291	0.325	0.368	0.420	0.147	0.167	0.164	0.189
	MAE	0.406	0.409	0.409	0.462	0.341	0.360	0.391	0.426	0.225	0.239	0.267	0.281
$k = 9$	MSE	0.386	0.413	0.407	0.474	0.302	0.349	0.403	0.419	0.157	0.189	0.194	0.212
	MAE	0.437	0.444	0.439	0.485	0.372	0.396	0.410	0.432	0.230	0.271	0.285	0.314

D.2 TRANING PROCESS HYPERPARAMETERS

Furthermore, acknowledging that hyperparameters such as learning rate and batch size influence the results, we present experimental results inclusive of standard deviation. We explore batch sizes ranging from 32 to 512, learning rates from 10^{-5} to 0.05, five seeds(1111,333,2023,2024,2025), and training epochs from 10 to 100. The findings are summarized in Table 19,Table 20 and Table21 for long-term forecasting,short-term forecasting and Anomaly detection.From the above results, we can find that for different training process Settings, the standard deviation of the results of different time series tasks is smaller, indicating that the model shows high robustness for different training Settings.

Table 19: Detailed performance of TVNet. We report MSE/MAE and standard deviation of different forecasting horizons $\{24, 36, 48, 60\}$ for ILI and $\{96, 192, 336, 720\}$ for others.$H1, H2, H3, H4$ means the horizons.

Horizon	Electricity		ETTh2		Exchange	
	MSE	MAE	MSE	MAE	MSE	MAE
$H1$	0.142 ± 0.002	0.223 ± 0.003	0.263 ± 0.003	0.329 ± 0.003	0.080 ± 0.002	0.195 ± 0.003
$H2$	0.165 ± 0.002	0.241 ± 0.006	0.319 ± 0.003	0.372 ± 0.002	0.163 ± 0.004	0.285 ± 0.002
$H3$	0.164 ± 0.003	0.269 ± 0.002	0.311 ± 0.004	0.373 ± 0.002	0.291 ± 0.003	0.394 ± 0.003
$H4$	0.190 ± 0.005	0.284 ± 0.002	0.401 ± 0.003	0.434 ± 0.004	0.658 ± 0.007	0.594 ± 0.002
Horizon	ILI		Traffic		Weather	
	MSE	MAE	MSE	MAE	MSE	MAE
$H1$	1.324 ± 0.006	0.712 ± 0.004	0.367 ± 0.003	0.252 ± 0.003	0.147 ± 0.005	0.198 ± 0.004
$H2$	1.190 ± 0.020	0.772 ± 0.018	0.381 ± 0.003	0.262 ± 0.004	0.194 ± 0.003	0.238 ± 0.003
$H3$	1.456 ± 0.015	0.782 ± 0.004	0.395 ± 0.004	0.268 ± 0.003	0.235 ± 0.005	0.277 ± 0.005
$H4$	1.652 ± 0.022	0.796 ± 0.005	0.442 ± 0.004	0.290 ± 0.006	0.308 ± 0.003	0.331 ± 0.003

Table 20: Detailed performance of TVNet. We report standard deviation on short-term forecasting

Models	Metrics	Yearly			Quarterly			Monthly			Others		
		SMAPE	MASE	OWA	SMAEP	MASE	OWA	SMAPE	MASE	OWA	SMAPE	MASE	OWA
TVNet		13.217 ± 0.005	2.899 ± 0.001	0.768 ± 0.004	9.986 ± 0.005	1.159 ± 0.002	0.876 ± 0.003	12.493 ± 0.003	0.921 ± 0.001	0.866 ± 0.002	4.764 ± 0.002	2.986 ± 0.002	0.969 ± 0.001

Table 21: Detailed performance of TVNet. We report standard deviation on Anomaly detection(F1)

Dataset	Model	SMD	MSL	SMAP	SWaT	PSM
Anomaly Detection(F1)	**Ours**	85.75 ± 0.06	85.16 ± 0.04	71.64 ± 00.03	93.72 ± 0.05	97.53 ± 0.09
Anomaly Detection(R)	**Ours**	83.49 ± 0.02	86.47 ± 0.03	58.26 ± 0.02	96.33 ± 0.05	96.76 ± 0.04
Anomaly Detection(P)	**Ours**	88.03 ± 0.03	83.91 ± 0.05	92.64 ± 0.06	91.26 ± 0.04	98.30 ± 0.04

E MORE ABLATION EXPERIMENTS

E.1 INTER-POOL MODULE

In this section, we further conducted ablation studies on the tasks of short-term forecasting and time series anomaly detection, and presented the results.(Table 23)

E.2 RESHAPE REPRESENTATION

The existing representations for time series include 1D, 2D (inter-pool, cross-dimensions), and 3D (inter-pool, intra-pool, and cross-dimensions). To demonstrate the effectiveness of the 3D-embedding(③) proposed in this paper, 1D-embedding$X_{emb} \in \mathcal{R}^{L \times C_m}$(label ①)and 2D-embedding $X_{emb} \in \mathcal{R}^{N \times P \times C_m}$(label ②) are designed following the same rationale.For the time series analysis task using **fixed weight convolution** for different methods, long-term forecasting(Prediction length =192) is tested.Table 24 shows the result.It can be seen from the results that the error is smaller than that of 1D-Embedding and 2D-Embedding.3D-Embedding, indicating that 3D-Embedding can better represent time series.

Table 22: Ablation of Inter-pool Module.(Anomaly detection(F1) and Short-term forecasting(OWA)

Dataset	Model	SMD	MSL	SMAP	SWaT	PSM
Anomaly Detection	**Ours**	85.75	85.16	71.64	93.72	97.53
	w/o	78.61	67.34	59.82	82.74	86.27
Dataset	Model	Yearly	Quarterly	Monthly	Others	
Short-term forecasting	**Ours**	0.768	0.876	0.866	0.969	
	w/o	0.809	1.231	0.929	1.205	

Table 23: Different Embedding ways for Anomaly-detection and short-term forecasting.

Dataset	Model	SMD	MSL	SMAP	SWaT	PSM
Anomaly Detection	①	67.38	70.29	65.43	75.41	85.77
	②	70.60	65.95	52.09	76.54	82.05
	③	80.21	83.24	69.41	87.65	92.34
Dataset	Model	Yearly	Quarterly	Monthly	Others	
Short-term forecasting	①	1.043	1.576	1.132	1.574	
	②	0.904	1.589	1.076	1.322	
	③	0.839	1.375	1.034	1.323	

Table 24: Different Embedding ways for long-term forecasting.

Embedding	Electricity		ETTh2		Exchange	
	MSE	MAE	MSE	MAE	MSE	MAE
①	0.214	0.318	0.347	0.391	0.185	0.320
②	0.209	0.304	0.333	0.386	0.171	0.312
③	**0.201**	**0.296**	**0.330**	**0.381**	**0.164**	**0.296**
Embedding	ETTm1		Traffic		Weather	
	MSE	MAE	MSE	MAE	MSE	MAE
①	0.357	0.392	0.440	0.349	0.271	0.292
②	0.332	0.383	0.427	0.320	0.262	0.271
③	**0.336**	**0.385**	**0.423**	**0.313**	**0.257**	**0.269**

E.3 Training speed and Memory

Considering that the hyperparameters set during different training processes and the look-back window can affect the number of model parameters and running speed, to make a fairer comparison of the parameters and training speed of different models, we selected three typical models: PatchTST (Transformer-based), Dlinear (MLP-based), and ModernTCN (CNN-based), as well as the model proposed in this paper for comparison. We unified the training hyperparameters as shown in Table 11. The results for different input lengths on ETTm2 (prediction length fixed at 96) are shown in Figure 15. From the figure, it can be observed that in terms of running speed, as the input length increases, the training time of PatchTST increases, and the memory usage of ModernTCN increases significantly. In contrast, the training time and memory usage of the TVNet proposed in this paper increase slowly with the increase of input length, proving the superiority of the proposed model in terms of efficiency and effectiveness.

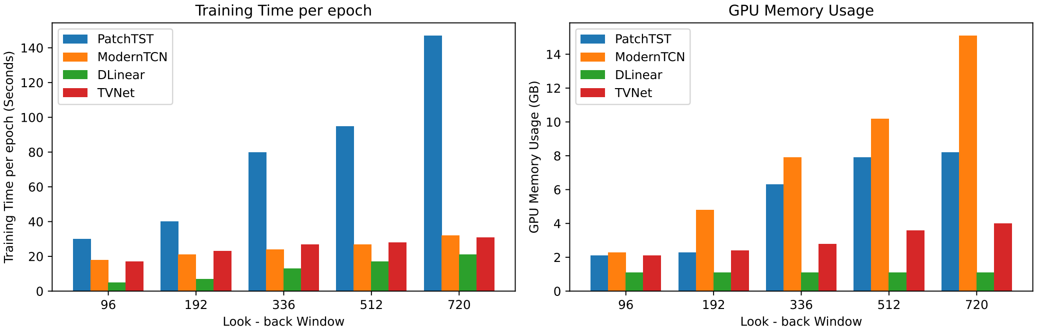

Figure 15: Params and GPU Memory for different input length(ETTm2)

F More Extra experiments studies

We have conducted additional experiments and analyses.

F.1 Input length

Impact of input length: In time series forecasting, the input length dictates the extent of historical data available for the algorithm's analysis. Typically, models that excel at capturing long-term dependencies tend to exhibit superior performance with increasing input lengths. To substantiate this, we evaluated our model across a range of input lengths while maintaining constant prediction lengths. Figure 16 illustrates that the performance of transformer-based models diminishes with longer inputs due to the prevalence of repetitive short-term patterns. Conversely, TVNet's predictive accuracy consistently improves with extended input lengths, suggesting its proficiency in capturing long-term dependencies and extracting meaningful information effectively.

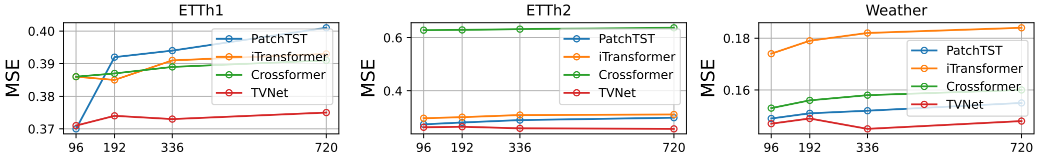

Figure 16: The MSE results with different input lengths and same prediction lengths(ETTh1,ETTh2 and Weather) prediction length(L)=192

F.2 Model robustness

We employ a straightforward noise injection technique to ascertain the robustness of our model. Specifically, we randomly select a proportion ϵ of data from the original input sequence and introduce random perturbations within the range $[-2X_i, 2X_i]$, where X_i represents the original data values. The perturbed data is subsequently utilized for training, and the mean squared error (MSE) and mean absolute error (MAE) metrics are documented. The findings are presented in Table 25. An increase in the perturbation ratio ϵ leads to a marginal rise in both MSE and MAE, indicating that TVNet demonstrates commendable robustness against mild noise (up to 10%) and excels at handling significant data anomalies, such as those caused by equipment malfunctions in power data.

Table 25: Different ϵ indicates different proportions of noise injection.

Models	Metrics	Weather				Electricity				Traffic			
		96	192	336	720	96	192	336	720	96	192	336	720
TVNet	MSE	0.147	0.194	0.235	0.308	0.142	0.165	0.164	0.190	0.367	0.381	0.395	0.442
	MAE	0.198	0.238	0.277	0.331	0.223	0.241	0.269	0.284	0.252	0.262	0.268	0.290
$\epsilon = 1\%$	MSE	0.146	0.192	0.238	0.305	0.142	0.165	0.167	0.191	0.365	0.382	0.396	0.444
	MAE	0.197	0.236	0.280	0.332	0.225	0.244	0.271	0.286	0.255	0.260	0.267	0.292
$\epsilon = 5\%$	MSE	0.150	0.196	0.238	0.307	0.148	0.170	0.166	0.191	0.369	0.380	0.399	0.445
	MAE	0.195	0.239	0.281	0.335	0.227	0.248	0.271	0.283	0.257	0.260	0.273	0.290
$\epsilon = 10\%$	MSE	0.159	0.207	0.245	0.310	0.149	0.176	0.177	0.194	0.379	0.386	0.405	0.451
	MAE	0.205	0.247	0.289	0.336	0.229	0.24 5	0.279	0.283	0.265	0.271	0.278	0.294

F.3 Univariate long-term forecasting results

Table 26 shows the Univariate long-term forecasting results.

Table 26: Following PatchTS(Nie et al., 2022) input length is fixed as 336 and prediction lengths are $T \in \{96, 192, 336, 720\}$. The best results are in **bold**.

Models	Metrics	TVNet		PatchTST		DLinear		FEDformer		Autoformer		Informer		LogTrans	
		MSE	MAE	MSE	MAE	MSE	MAE	MSE	MAE	MSE	MAE	MSE	MAE	MSE	MAE
ETTh1	96	**0.053**	**0.179**	0.055	0.179	0.056	0.180	0.079	0.215	0.071	0.206	0.193	0.377	0.283	0.468
	192	**0.067**	**0.202**	0.071	0.205	0.071	0.204	0.104	0.245	0.114	0.262	0.217	0.295	0.234	0.409
	336	**0.071**	**0.210**	0.076	0.220	0.098	0.244	0.119	0.270	0.107	0.258	0.202	0.381	0.286	0.546
	720	**0.083**	**0.229**	0.087	0.236	0.087	0.359	0.142	0.299	0.126	0.283	0.183	0.355	0.475	0.629
ETTh2	96	**0.121**	**0.268**	0.129	0.282	0.131	0.279	0.128	0.271	0.153	0.306	0.213	0.373	0.217	0.379
	192	**0.164**	**0.320**	0.168	0.328	0.176	0.329	0.185	0.330	0.204	0.351	0.227	0.387	0.281	0.429
	336	**0.171**	**0.333**	0.171	0.336	0.209	0.367	0.231	0.378	0.246	0.389	0.242	0.408	0.293	0.437
	720	**0.219**	**0.380**	0.223	0.380	0.276	0.426	0.278	0.420	0.268	0.409	0.291	0.439	0.218	0.387
ETTm1	96	**0.024**	**0.120**	0.026	0.121	0.028	0.123	0.033	0.140	0.056	0.183	0.109	0.277	0.218	0.387
	192	**0.038**	**0.150**	0.039	0.150	0.045	0.156	0.058	0.186	0.081	0.216	0.151	0.310	0.157	0.317
	336	**0.053**	**0.173**	0.053	0.173	0.061	0.182	0.084	0.231	0.076	0.218	0.427	0.591	0.289	0.459
	720	**0.072**	**0.203**	0.073	0.206	0.080	0.210	0.102	0.250	0.110	0.267	0.438	0.586	0.430	0.579
ETTm2	96	**0.063**	**0.183**	0.065	0.186	0.063	0.183	0.067	0.198	0.065	0.189	0.088	0.225	0.075	0.208
	192	**0.089**	**0.227**	0.093	0.231	0.092	0.227	0.102	0.245	0.118	0.256	0.132	0.283	0.129	0.275
	336	**0.119**	**0.261**	0.120	0.265	0.119	0.261	0.130	0.279	0.154	0.305	0.180	0.336	0.154	0.302
	720	**0.170**	**0.322**	0.171	0.322	0.175	0.320	0.178	0.325	0.182	0.335	0.300	0.435	0.160	0.321

F.4 LLM AND MORE BASELINES

For the long-term forecasting task, we have added some new Baselines (LLM-Based and TMixer). Table 27 shows the results, from which we can see that TVNet has shown good performance in most of the forecasting results.

Table 27: The complete results for **long-term forecasting** are detailed(More baselines focused on LLM), demonstrating a thorough comparison among various competitive models across four distinct forecast horizons.The Avg metric indicates the average performance across these forecast horizons.

Models		**TVNet** (Ours)		S2IP-LLM (2024)		TimeLLM (2023)		GPT4TS (2024)		TimeMixer (2024b)	
Metrics		MSE	MAE	MSE	MAE	MSE	MAE	MSE	MAE	MSE	MAE
ETTm1	96	**0.288**	**0.343**	0.288	0.346	0.311	0.365	0.292	0.346	0.320	0.357
	192	0.326	0.367	**0.323**	**0.365**	0.364	0.395	0.332	0.372	0.361	0.381
	336	0.365	0.391	**0.359**	**0.390**	0.369	0.398	0.366	0.394	0.390	0.404
	720	0.412	**0.413**	**0.403**	0.418	0.416	0.425	0.417	0.421	0.454	0.441
	Avg	0.348	**0.379**	**0.343**	0.379	0.365	0.395	0.388	0.403	0.381	0.395
ETTm2	96	**0.161**	**0.254**	0.165	0.257	0.170	0.262	0.173	0.262	0.175	0.258
	192	**0.220**	**0.293**	0.222	0.299	0.229	0.303	0.229	0.301	0.237	0.299
	336	**0.272**	**0.316**	0.277	0.330	0.281	0.335	0.286	0.341	0.298	0.340
	720	**0.349**	**0.379**	0.363	0.390	0.379	0.403	0.378	0.401	0.391	0.396
	Avg	**0.251**	**0.311**	0.257	0.319	0.264	0.325	0.284	0.339	0.275	0.323
ETTh1	96	0.371	0.408	**0.366**	**0.396**	0.380	0.406	0.376	0.397	0.375	0.400
	192	**0.398**	**0.409**	0.401	0.420	0.426	0.438	0.416	0.418	0.429	0.421
	336	**0.401**	**0.409**	0.412	0.431	0.437	0.451	0.442	0.433	0.484	0.458
	720	0.458	0.459	**0.440**	**0.458**	0.515	0.509	0.477	0.456	0.498	0.482
	Avg	0.407	**0.421**	**0.406**	0.427	0.439	0.451	0.465	0.455	0.447	0.440
ETTh2	96	**0.263**	**0.329**	0.278	0.340	0.306	0.362	0.285	0.342	0.289	0.341
	192	**0.319**	**0.372**	0.346	0.385	0.346	0.385	0.354	0.389	0.372	0.392
	336	**0.311**	**0.373**	0.367	0.406	0.393	0.422	0.373	0.407	0.386	0.414
	720	0.401	0.434	0.400	0.436	**0.397**	**0.433**	0.406	0.441	0.412	0.434
	Avg	**0.324**	**0.377**	0.347	0.391	0.360	0.400	0.381	0.412	0.364	0.395
Electricity	96	0.142	**0.223**	**0.135**	0.230	0.140	0.246	0.139	0.238	0.153	0.247
	192	0.165	**0.241**	**0.149**	0.247	0.155	0.253	0.153	0.251	0.166	0.256
	336	**0.164**	0.269	0.167	**0.266**	0.175	0.279	0.169	0.266	0.185	0.277
	720	**0.190**	**0.284**	0.200	0.287	0.204	0.305	0.206	0.297	0.225	0.310
	Avg	0.165	**0.254**	**0.161**	0.257	0.168	0.270	0.167	0.263	0.182	0.272
Weather	96	0.147	0.198	**0.145**	**0.195**	0.148	0.197	0.162	0.212	0.163	0.209
	192	0.194	0.238	**0.190**	**0.235**	0.194	0.246	0.204	0.248	0.208	0.250
	336	**0.235**	**0.277**	0.243	0.280	0.248	0.285	0.254	0.286	0.251	0.287
	720	**0.308**	**0.331**	0.312	0.326	0.317	0.332	0.326	0.337	0.339	0.341
	Avg	**0.221**	0.261	0.222	**0.259**	0.226	0.265	0.237	0.270	0.240	0.271
Traffic	96	**0.367**	**0.252**	0.379	0.274	0.383	0.280	0.388	0.282	0.462	0.285
	192	**0.381**	**0.262**	0.397	0.282	0.399	0.294	0.407	0.290	0.473	0.296
	336	**0.395**	**0.268**	0.407	0.289	0.411	0.306	0.412	0.294	0.498	0.296
	720	0.442	**0.290**	0.440	0.301	0.448	0.319	0.450	0.312	0.506	0.313
	Avg	**0.396**	**0.268**	0.405	0.286	0.440	0.301	0.414	0.294	0.484	0.297

F.5 EXOGENOUS VARIABLE FORECASTING

As discussed in Timexer (Wang et al., 2024b), forecasting exogenous variables is crucial in various domains, including load forecasting. Our experiments on the ETT dataset also focused on predicting such variables. Figures 17 demonstrate that TVNet consistently outperforms the optimal baseline model in exogenous variable forecasting.

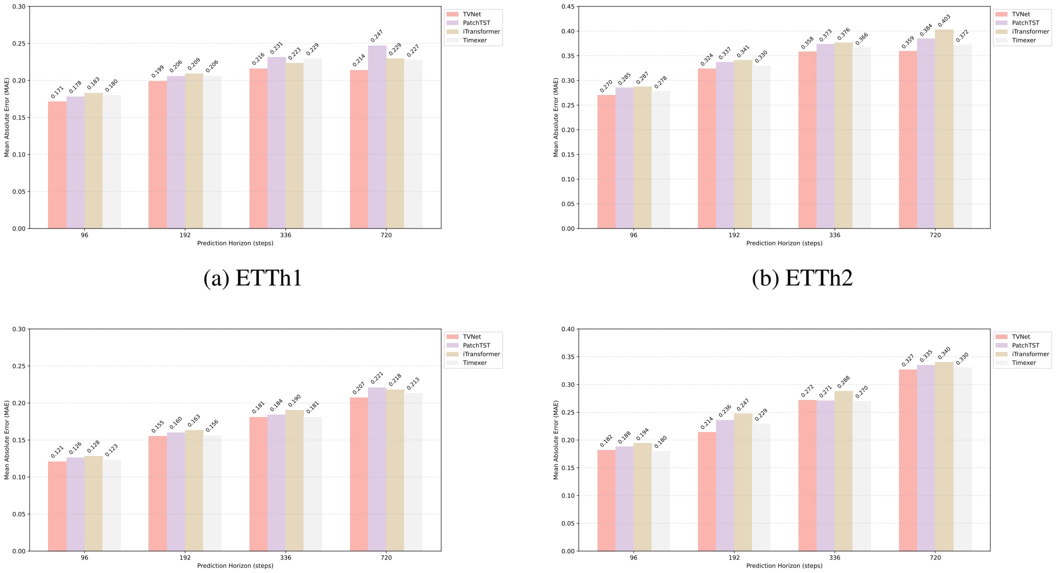

(a) ETTh1

(b) ETTh2

(c) ETTm1

(d) ETTm2

Figure 17: Exogenous variable learning results for ETT dataset.

G Full results

G.1 Long-term forecasting

Table 28: The complete results for **long-term forecasting** are detailed, demonstrating a thorough comparison among various competitive models across four distinct forecast horizons.The Avg metric indicates the average performance across these forecast horizons.

Models		**TVNet**		PatchTST		iTransformer		Crossformer		RLinear		MTS-Mixer		DLinear		TimesNet		MICN		ModernTCN		FEDformer		RMLP	
		(Ours)		(2022)		(2023)		(2023)		(2023a)		(2023b)		(2023b)		(2022a)		(2023)		(2024)		(2022)		(2023a)	
Metrics		MSE	MAE	MSE	MAE	MSE	MAE	MSE	MAE	MSE	MAE	MSE	MAE	MSE	MAE	MSE	MAE	MSE	MAE	MSE	MAE	MSE	MAE	MSE	MAE
ETTm1	96	**0.288**	0.343	0.290	**0.342**	0.334	0.368	0.316	0.373	0.301	0.342	0.314	0.358	0.299	0.343	0.338	0.375	0.314	0.360	0.292	0.346	0.326	0.390	0.298	0.345
	192	**0.326**	**0.367**	0.332	0.369	0.377	0.391	0.377	0.411	0.355	0.363	0.354	0.386	0.335	0.365	0.371	0.387	0.359	0.387	0.332	0.368	0.365	0.415	0.344	0.375
	336	**0.365**	**0.391**	0.366	0.392	0.426	0.420	0.431	0.442	0.370	0.383	0.384	0.405	0.369	0.386	0.410	0.411	0.398	0.413	**0.365**	**0.391**	0.392	0.425	0.390	0.410
	720	**0.412**	**0.413**	0.416	0.420	0.491	0.459	0.600	0.547	0.425	0.414	0.427	0.432	0.425	0.421	0.478	0.450	0.459	0.464	0.416	0.417	0.446	0.458	0.445	0.441
	Avg	**0.348**	**0.379**	0.351	0.381	0.407	0.410	0.431	0.443	0.358	0.376	0.370	0.395	0.357	0.379	0.400	0.450	0.383	0.406	0.351	0.381	0.382	0.422	0.369	0.393
ETTm2	96	**0.161**	**0.254**	0.165	0.255	0.180	0.264	0.421	0.461	0.164	0.253	0.177	0.259	0.167	0.260	0.187	0.267	0.178	0.273	0.166	0.256	0.180	0.271	0.174	0.259
	192	0.220	0.293	0.220	0.292	0.250	0.309	0.503	0.519	**0.219**	**0.290**	0.241	0.303	0.224	0.303	0.249	0.309	0.245	0.316	0.222	0.293	0.252	0.318	0.236	0.303
	336	**0.272**	**0.316**	0.274	0.329	0.311	0.348	0.611	0.580	0.273	0.326	0.297	0.338	0.281	0.342	0.312	0.351	0.295	0.350	**0.272**	0.324	0.324	0.364	0.291	0.338
	720	**0.349**	**0.379**	0.362	0.385	0.412	0.407	0.996	0.750	0.366	0.385	0.396	0.398	0.397	0.421	0.497	0.403	0.389	0.406	0.351	0.381	0.410	0.420	0.371	0.391
	Avg	**0.251**	**0.311**	0.255	0.315	0.288	0.332	0.632	0.578	0.256	0.314	0.277	0.325	0.267	0.332	0.291	0.333	0.277	0.336	0.253	0.314	0.292	0.343	0.268	0.322
ETTh1	96	0.371	0.408	0.370	0.399	0.386	0.405	0.386	0.429	0.366	0.391	0.372	0.395	0.375	0.399	0.384	0.402	0.396	0.427	**0.368**	**0.394**	0.376	0.415	0.390	0.410
	192	**0.398**	**0.409**	0.413	0.421	0.441	0.436	0.419	0.444	0.404	0.412	0.416	0.426	0.405	0.416	0.557	0.436	0.430	0.453	0.405	0.413	0.423	0.446	0.430	0.432
	336	0.401	0.409	0.422	0.436	0.487	0.458	0.440	0.461	0.420	0.423	0.455	0.449	0.439	0.443	0.491	0.469	0.433	0.458	**0.391**	**0.412**	0.444	0.462	0.441	0.441
	720	0.458	**0.459**	**0.447**	0.466	0.503	0.491	0.519	0.524	0.442	0.456	0.475	0.472	0.472	0.490	0.521	0.500	0.474	0.508	0.450	0.461	0.469	0.492	0.506	0.495
	Avg	0.407	0.421	0.413	0.431	0.454	0.447	0.441	0.465	0.408	0.421	0.430	0.436	0.423	0.437	0.458	0.450	0.433	0.462	**0.404**	**0.420**	0.428	0.454	0.442	0.445
ETTh2	96	0.263	**0.329**	0.274	0.336	0.297	0.349	0.628	0.563	**0.262**	0.331	0.307	0.354	0.289	0.353	0.340	0.374	0.289	0.357	0.263	0.332	0.332	0.374	0.288	0.352
	192	**0.319**	**0.372**	0.339	0.379	0.380	0.400	0.703	0.624	0.320	0.374	0.374	0.399	0.383	0.418	0.402	0.414	0.409	0.438	0.320	0.374	0.407	0.446	0.343	0.387
	336	**0.311**	**0.373**	0.329	0.380	0.428	0.432	0.827	0.675	0.325	0.386	0.398	0.432	0.448	0.465	0.452	0.452	0.417	0.452	0.313	0.376	0.400	0.447	0.353	0.402
	720	0.401	0.434	0.379	0.422	0.427	0.445	1.181	0.840	**0.372**	**0.421**	0.463	0.465	0.605	0.551	0.462	0.468	0.426	0.473	0.392	0.433	0.412	0.469	0.410	0.440
	Avg	0.324	0.377	0.330	0.379	0.383	0.407	0.835	0.676	**0.320**	**0.378**	0.386	0.413	0.431	0.447	0.414	0.427	0.385	0.430	0.322	0.379	0.388	0.434	0.349	0.395
Electricity	96	0.142	0.223	**0.129**	**0.222**	0.148	0.240	0.187	0.283	0.140	0.235	0.141	0.243	0.153	0.237	0.168	0.272	0.159	0.267	0.129	0.226	0.186	0.302	0.129	0.224
	192	0.165	0.241	0.147	0.240	0.162	0.253	0.258	0.330	0.154	0.248	0.163	0.261	0.152	0.249	0.184	0.289	0.168	0.279	**0.143**	**0.239**	0.197	0.311	0.147	0.240
	336	0.164	0.269	0.163	0.259	0.178	0.269	0.323	0.369	0.171	0.264	0.176	0.277	0.169	0.267	0.198	0.300	0.196	0.308	**0.161**	**0.259**	0.213	0.328	0.164	0.257
	720	**0.190**	**0.284**	0.197	0.290	0.225	0.317	0.404	0.423	0.209	0.297	0.212	0.308	0.233	0.344	0.220	0.320	0.203	0.312	0.191	0.286	0.233	0.344	0.203	0.291
	Avg	0.165	0.254	0.159	**0.253**	0.178	0.270	0.293	0.351	0.169	0.261	0.173	0.272	0.177	0.274	0.192	0.295	0.182	0.292	**0.156**	**0.253**	0.207	0.321	0.161	**0.253**
Weather	96	**0.147**	**0.198**	0.149	0.198	0.174	0.214	0.153	0.217	0.175	0.225	0.156	0.206	0.152	0.237	0.172	0.220	0.161	0.226	0.149	0.200	0.238	0.314	0.149	0.202
	192	**0.194**	**0.238**	0.194	0.241	0.221	0.254	0.197	0.269	0.218	0.260	0.199	0.248	0.220	0.282	0.219	0.261	0.220	0.283	0.196	0.245	0.275	0.329	0.194	0.242
	336	**0.235**	**0.277**	0.245	0.282	0.278	0.296	0.252	0.311	0.265	0.294	0.249	0.291	0.265	0.319	0.280	0.306	0.275	0.328	0.238	0.277	0.339	0.377	0.243	0.282
	720	**0.308**	**0.331**	0.314	0.334	0.358	0.347	0.318	0.363	0.329	0.339	0.336	0.343	0.323	0.362	0.365	0.359	0.311	0.356	0.314	0.334	0.389	0.409	0.316	0.333
	Avg	**0.221**	**0.261**	0.226	0.264	0.258	0.278	0.230	0.290	0.247	0.279	0.235	0.272	0.240	0.300	0.259	0.287	0.242	0.298	0.224	0.264	0.310	0.357	0.225	0.265
Traffic	96	0.367	0.252	**0.360**	**0.249**	0.395	0.268	0.512	0.290	0.496	0.375	0.462	0.332	0.410	0.282	0.593	0.321	0.508	0.301	0.368	0.253	0.576	0.359	0.430	0.327
	192	0.381	0.262	**0.379**	**0.256**	0.417	0.276	0.523	0.297	0.503	0.377	0.488	0.354	0.423	0.287	0.617	0.336	0.536	0.315	**0.379**	0.261	0.610	0.380	0.451	0.340
	336	0.395	0.268	**0.392**	**0.264**	0.433	0.283	0.530	0.300	0.517	0.382	0.498	0.360	0.436	0.296	0.629	0.336	0.525	0.310	0.397	0.270	0.608	0.375	0.470	0.351
	720	0.442	0.290	**0.432**	**0.286**	0.467	0.302	0.573	0.313	0.555	0.398	0.529	0.370	0.466	0.315	0.640	0.350	0.571	0.323	0.440	0.296	0.621	0.375	0.513	0.372
	Avg	0.396	0.268	**0.391**	**0.264**	0.428	0.282	0.535	0.300	0.518	0.383	0.494	0.354	0.434	0.295	0.620	0.336	0.535	0.312	0.396	0.270	0.604	0.372	0.466	0.348
Exchange	96	**0.080**	**0.195**	0.093	0.214	0.086	0.206	0.186	0.346	0.083	0.301	0.083	0.020	0.081	0.203	0.107	0.234	0.102	0.235	0.080	0.196	0.139	0.276	0.083	0.201
	192	0.163	**0.285**	0.192	0.312	0.177	0.299	0.467	0.522	0.170	0.293	0.174	0.296	**0.157**	0.293	0.226	0.344	0.172	0.316	0.166	0.288	0.256	0.369	0.170	0.292
	336	0.291	**0.394**	0.350	0.432	0.331	0.417	0.783	0.721	0.309	0.401	0.336	0.417	0.305	0.414	0.367	0.448	**0.272**	0.407	0.307	0.398	0.426	0.464	0.309	0.401
	720	0.658	0.594	0.911	0.716	0.847	0.691	1.367	0.943	0.817	0.680	0.900	0.715	**0.643**	0.601	0.964	0.746	0.714	0.658	0.656	**0.582**	1.090	0.800	0.816	0.680
	Avg	0.298	0.367	0.387	0.419	0.360	0.403	0.701	0.633	0.345	0.394	0.373	0.407	**0.297**	0.378	0.416	0.443	0.315	0.404	0.302	**0.366**	0.478	0.478	0.345	0.394
ILI	24	1.324	**0.712**	**1.319**	0.754	2.207	1.032	3.040	1.186	4.337	1.507	1.472	0.798	2.215	1.081	2.317	0.934	2.684	1.112	1.347	0.717	2.624	1.095	4.445	1.536
	36	**1.190**	**0.772**	1.430	0.834	1.934	0.951	3.356	1.230	4.205	1.481	1.435	0.745	1.963	0.963	1.972	0.920	2.507	1.013	1.250	0.778	2.516	1.021	4.409	1.159
	48	1.456	0.782	1.553	0.815	2.127	1.004	3.441	1.223	4.257	1.484	1.474	0.822	2.130	1.024	2.238	0.940	2.423	1.012	**1.388**	**0.781**	2.505	1.041	4.388	1.507
	60	1.652	0.796	**1.470**	**0.788**	2.298	0.998	3.608	1.302	4.278	1.487	1.839	0.912	2.368	1.096	2.027	0.928	2.653	1.085	1.774	0.868	2.742	1.122	4.306	1.502
	Avg	**1.406**	**0.766**	1.443	0.798	2.141	0.996	3.361	1.235	4.269	1.490	1.555	0.819	2.169	1.041	2.139	0.931	2.567	1.055	1.440	0.786	2.597	1.070	4.387	1.516
	1st count	**21**	**24**	9	9	0	0	0	0	4	3	0	0	3	0	0	0	1	0	11	12	0	0	0	1

G.2 Short-term Forecasting

Table 29: The complete results for the **short-term forecasting** task in the M4 dataset are presented, utilizing the Weighted Average (WA) as the metric.

Models		**TVNet** (Ours)	PatchTST (2022)	U-Mixer (2024)	Crossformer (2023)	RLinear (2023a)	MTS-Mixer (2023b)	DLinear (2023)	TimesNet (2022a)	MICN 2023)	ModernTCN (2024)	FEDformer (2022)	N-HiTS (2023)
Yearly	SMAPE	**13.217**	13.258	13.317	13.392	13.944	13.548	16.965	13.387	14.935	13.226	13.728	13.418
	MASE	**2.899**	2.985	3.006	3.001	3.015	3.091	4.283	2.996	3.523	2.957	3.048	3.045
	OWA	**0.768**	0.781	0.786	0.787	0.807	0.803	1.058	0.786	0.900	0.777	0.803	0.793
Quarterly	SMAPE	9.986	10.197	9.956	16.317	10.702	10.128	12.145	10.100	11.452	**9.971**	10.792	10.202
	MASE	**1.159**	0.803	1.156	2.197	1.299	1.196	1.520	1.182	1.389	1.167	1.283	1.194
	OWA	**0.876**	0.803	0.873	1.542	0.959	0.896	1.106	0.890	1.026	0.878	0.958	0.899
Monthly	SMAPE	**12.493**	12.641	13.057	12.924	13.363	12.717	13.514	12.670	13.773	12.556	14.260	12.791
	MASE	0.921	0.930	1.067	0.966	1.014	0.931	1.037	0.933	1.076	**0.917**	1.102	0.969
	OWA	**0.866**	0.876	0.976	0.902	0.940	0.879	0.956	0.878	0.983	0.866	1.012	0.899
Others	SMAPE	4.764	4.946	4.858	5.493	5.437	4.817	6.709	4.891	6.716	**4.715**	4.954	5.061
	MASE	2.986	**2.985**	3.195	3.690	3.706	3.255	4.953	3.302	4.717	3.107	3.264	3.216
	OWA	**0.969**	1.044	1.015	1.160	1.157	1.02	1.487	1.035	1.451	0.986	1.036	1.040
WA	SMAPE	**11.671**	11.807	11.740	13.474	12.473	11.892	13.639	11.829	13.130	11.698	12.840	11.927
	MASE	**1.536**	1.590	1.575	1.866	1.677	1.608	2.095	1.585	1.896	11.556	1.701	1.613
	OWA	**0.832**	0.851	0.845	0.985	0.898	0.859	1.051	0.851	0.980	0.838	0.918	0.861

G.3 Imputation

Table 30: The complete results for the **imputation task** are as follows: To assess model performance under varying degrees of missing data, we randomly masked time points at rates of 12.5%, 25%, 37.5%, and 50%.

Models		**TVNet** (Ours)		PatchTST (2022)		SCINet (2022a)		Crossformer (2023)		RLinear (2023a)		MTS-Mixer (2023b)		DLinear (2023)		TimesNet (2022a)		MICN 2023)		ModernTCN (2024)		FEDformer (2022)		RMLP (2023a)	
Metrics		MSE	MAE	MSE	MAE	MSE	MAE	MSE	MAE	MSE	MAE	MSE	MAE	MSE	MAE	MSE	MAE	MSE	MAE	MSE	MAE	MSE	MAE	MSE	MAE
ETTm1	12.5%	**0.014**	**0.078**	0.041	0.128	0.031	0.116	0.037	0.137	0.047	0.137	0.043	0.134	0.058	0.162	0.019	0.092	0.039	0.137	0.015	0.082	0.035	0.135	0.049	0.139
	25%	**0.016**	**0.083**	0.043	0.130	0.036	0.124	0.038	0.141	0.061	0.157	0.051	0.147	0.080	0.193	0.023	0.101	0.059	0.170	0.018	0.088	0.052	0.166	0.057	0.154
	37.5%	**0.019**	**0.090**	0.044	0.133	0.041	0.134	0.041	0.142	0.077	0.175	0.060	0.160	0.103	0.219	0.029	0.111	0.080	0.199	0.021	0.095	0.069	0.191	0.067	0.168
	50%	**0.023**	**0.101**	0.050	0.142	0.049	0.143	0.047	0.152	0.096	0.195	0.070	0.174	0.132	0.248	0.036	0.124	0.103	0.221	0.026	0.105	0.089	0.218	0.079	0.183
	Avg	**0.018**	**0.088**	0.045	0.133	0.039	0.129	0.041	0.143	0.070	0.166	0.056	0.154	0.093	0.206	0.027	0.107	0.070	0.182	0.020	0.093	0.062	0.177	0.063	0.161
ETTm2	12.5%	0.018	0.081	0.025	0.092	0.023	0.093	0.044	0.148	0.026	0.093	0.026	0.096	0.062	0.166	0.018	0.080	0.060	0.165	**0.017**	**0.076**	0.056	0.159	0.026	0.096
	25%	0.021	0.081	0.027	0.095	0.026	0.100	0.047	0.151	0.030	0.103	0.030	0.103	0.085	0.196	0.020	0.085	0.100	0.216	**0.018**	**0.080**	0.080	0.195	0.030	0.106
	37.5%	0.025	0.089	0.029	0.099	0.028	0.105	0.044	0.145	0.034	0.113	0.033	0.110	0.106	0.222	0.023	0.091	0.163	0.273	**0.020**	**0.084**	0.110	0.231	0.034	0.113
	50%	0.024	0.091	0.032	0.106	0.031	0.111	0.047	0.150	0.039	0.123	0.037	0.118	0.131	0.247	0.026	0.098	0.254	0.342	**0.022**	**0.090**	0.156	0.276	0.039	0.121
	Avg	0.022	0.086	0.028	0.098	0.027	0.102	0.046	0.149	0.032	0.108	0.032	0.107	0.096	0.208	0.022	0.088	0.144	0.249	**0.019**	**0.082**	0.101	0.215	0.032	0.109
ETTh1	12.5%	**0.032**	**0.119**	0.094	0.199	0.089	0.202	0.099	0.218	0.098	0.206	0.097	0.209	0.151	0.267	0.057	0.159	0.072	0.192	0.035	0.128	0.070	0.190	0.096	0.205
	25%	**0.039**	**0.137**	0.119	0.225	0.099	0.211	0.125	0.243	0.123	0.229	0.115	0.226	0.180	0.292	0.069	0.178	0.105	0.232	0.042	0.140	0.106	0.236	0.120	0.228
	37.5%	**0.051**	**0.156**	0.145	0.248	0.107	0.218	0.146	0.263	0.153	0.253	0.135	0.244	0.215	0.318	0.084	0.196	0.139	0.267	0.054	0.157	0.124	0.258	0.145	0.250
	50%	**0.064**	**0.168**	0.173	0.271	0.120	0.231	0.158	0.281	0.188	0.278	0.160	0.263	0.257	0.347	0.102	0.215	0.185	0.310	0.067	0.174	0.165	0.299	0.176	0.274
	Avg	**0.046**	**0.145**	0.133	0.236	0.104	0.216	0.132	0.251	0.141	0.242	0.127	0.236	0.201	0.306	0.078	0.187	0.125	0.250	0.050	0.150	0.117	0.246	0.134	0.239
ETTh2	12.5%	**0.036**	**0.119**	0.057	0.150	0.061	0.161	0.103	0.220	0.057	0.152	0.061	0.157	0.100	0.216	0.040	0.130	0.106	0.223	0.037	0.121	0.095	0.212	0.058	0.153
	25%	**0.038**	**0.123**	0.062	0.158	0.062	0.162	0.110	0.229	0.062	0.160	0.065	0.163	0.127	0.247	0.046	0.141	0.151	0.271	0.040	0.127	0.137	0.258	0.064	0.161
	37.5%	**0.040**	**0.126**	0.068	0.168	0.065	0.166	0.129	0.246	0.068	0.168	0.070	0.171	0.158	0.276	0.052	0.151	0.229	0.332	0.043	0.134	0.187	0.304	0.070	0.171
	50%	**0.044**	**0.143**	0.076	0.179	0.069	0.172	0.148	0.265	0.076	0.179	0.078	0.181	0.183	0.299	0.060	0.162	0.334	0.403	0.048	0.143	0.232	0.341	0.078	0.181
	Avg	**0.039**	**0.127**	0.066	0.164	0.064	0.165	0.122	0.240	0.066	0.165	0.069	0.168	0.142	0.259	0.049	0.146	0.205	0.307	0.042	0.131	0.163	0.279	0.068	0.166
Electricity	12.5%	0.065	0.180	0.073	0.188	0.073	0.185	0.068	0.181	0.079	0.199	0.069	0.182	0.092	0.214	0.085	0.202	0.090	0.216	**0.059**	**0.171**	0.107	0.237	0.073	0.188
	25%	0.075	0.192	0.082	0.200	0.081	0.198	0.079	0.198	0.105	0.233	0.083	0.202	0.118	0.247	0.089	0.206	0.108	0.236	**0.071**	**0.188**	0.120	0.251	0.090	0.211
	37.5%	0.085	0.196	0.097	0.217	0.090	0.207	0.087	0.203	0.131	0.262	0.097	0.218	0.144	0.276	0.094	0.213	0.128	0.257	**0.077**	**0.190**	0.136	0.266	0.107	0.231
	50%	0.091	0.210	0.110	0.232	0.099	0.214	0.096	0.212	0.160	0.291	0.108	0.231	0.175	0.305	0.100	0.221	0.151	0.278	**0.085**	**0.200**	0.158	0.284	0.125	0.252
	Avg	0.079	0.194	0.091	0.209	0.086	0.201	0.083	0.199	0.119	0.246	0.089	0.208	0.132	0.260	0.092	0.210	0.119	0.247	**0.073**	**0.187**	0.130	0.259	0.099	0.221
Weather	12.5%	**0.021**	**0.037**	0.029	0.049	0.028	0.047	0.036	0.092	0.029	0.048	0.033	0.052	0.039	0.084	0.025	0.045	0.036	0.088	0.023	0.038	0.041	0.107	0.030	0.051
	25%	**0.024**	**0.037**	0.031	0.053	0.029	0.050	0.035	0.088	0.032	0.055	0.034	0.056	0.048	0.103	0.029	0.052	0.047	0.115	0.025	0.041	0.064	0.163	0.033	0.057
	37.5%	**0.024**	**0.040**	0.034	0.058	0.031	0.055	0.035	0.088	0.036	0.062	0.037	0.060	0.057	0.117	0.031	0.057	0.062	0.141	0.027	0.046	0.107	0.229	0.036	0.062
	50%	**0.028**	**0.041**	0.039	0.066	0.034	0.059	0.038	0.092	0.040	0.067	0.041	0.066	0.066	0.134	0.034	0.062	0.080	0.168	0.031	0.051	0.183	0.312	0.040	0.068
	Avg	**0.024**	**0.039**	0.033	0.057	0.031	0.053	0.036	0.090	0.034	0.058	0.036	0.058	0.052	0.110	0.030	0.054	0.056	0.128	0.027	0.044	0.099	0.203	0.035	0.060

G.4 Classification

Table 31: Performance comparison of various models on different datasets with accuracy metrics for **classification**.

Datasets / Models	RNN-based			Convolution-based				MLP-based			Transformer-based				
	LSTNet	LSSL	Rocket	SCINet	TimesNet	MICN	ModernTCN	DLinear	LightTS	MTS-Mixer	FED.	PatchTST	Cross.	Flow.	**TVNet**
	(2018)	(2021)	(2020)	(2022a)	2022a	(2023)	(2024)	(2023)	(2022)	(2023b)	(2022)	(2022)	(2023)	(2022b)	(Ours)
EthanolConcentration	39.9	31.1	45.2	34.4	35.3	35.7	36.3	36.2	29.7	33.8	31.2	32.8	38.0	33.8	35.6
FaceDetection	65.7	66.7	64.7	68.9	65.2	68.6	70.8	68.0	67.5	70.2	66.0	68.3	68.7	67.6	71.2
Handwriting	25.8	24.6	58.8	23.6	25.5	32.1	30.6	27.0	26.1	26.0	28.0	29.6	28.8	33.8	32.7
Heartbeat	77.1	72.7	75.6	77.5	74.7	78.0	77.2	75.1	75.1	77.1	73.7	74.9	77.6	77.6	78.1
JapaneseVowels	98.1	98.4	96.2	96.0	94.6	98.4	98.8	96.2	96.2	94.3	98.4	97.5	99.1	98.9	98.9
PEMS-SF	86.7	86.1	75.1	83.8	85.5	89.6	89.1	75.1	88.4	80.9	80.9	89.3	85.9	86.0	88.9
SelfRegulationSCP1	84.0	90.8	90.8	92.5	86.0	91.8	93.4	87.3	89.8	91.7	88.7	90.7	92.1	92.5	93.7
SelfRegulationSCP2	52.8	52.2	53.3	57.2	53.6	57.2	60.3	50.5	51.1	55.0	54.4	57.8	58.3	56.1	60.5
SpokenArabicDigits	100.0	100.0	71.2	98.1	97.1	99.0	98.7	81.4	100.0	97.4	100.0	98/3	97.9	98.8	99.4
UWaveGestureLibrary	87.8	85.9	94.4	85.1	82.8	85.3	86.7	82.1	80.3	82.3	85.3	85.8	85.3	86.6	86.6
Average Accuracy	71.8	70.9	72.5	71.7	70.0	73.6	74.2	67.5	70.4	70.9	70.7	72.5	73.2	73.0	**74.6**

G.5 Anomaly detection

Table 32: Performance comparison of various models on different datasets with Precision (P), Recall (R), and F1-score (F1) metrics for **annomaly detection**.

Models	Datasets	SMD			MSL			SMAP			SWaT			PSM			Avg F1
	Metrics	P	R	F1	P	R	F1	P	R	F1	P	R	F1	P	R	F1	(%)
SCINet	(2022a)	85.97	82.57	84.24	84.16	82.61	83.38	93.12	54.81	69.00	87.53	94.95	91.09	97.93	94.15	96.00	84.74
MICN	(2023)	88.45	83.47	85.89	83.02	83.67	83.34	90.65	61.42	73.23	91.87	95.08	93.45	98.40	88.69	93.29	85.84
TimesNet	(2022a)	88.66	83.14	85.81	83.92	86.32	85.15	92.52	58.29	71.52	86.76	97.32	91.74	98.19	96.76	97.47	86.34
DLinear	(2023)	83.62	71.52	77.10	84.34	84.52	84.88	92.32	55.41	69.26	80.91	95.30	87.52	98.28	89.26	93.55	82.46
LightTS	(2022)	87.10	78.42	82.53	82.40	75.78	78.95	92.58	55.27	69.21	91.98	94.72	93.33	98.37	95.97	97.15	84.23
MTS-Mixer	(2023b)	88.60	82.92	85.67	85.35	84.13	84.74	92.13	58.01	71.19	84.49	93.81	88.91	98.41	88.63	93.26	84.75
RLLinear	(2023a)	87.79	79.98	83.70	89.26	74.39	81.15	89.94	54.01	67.49	92.27	93.18	92.73	98.47	94.28	96.33	84.28
RMLP	(2023a)	87.35	78.10	82.46	86.67	65.30	74.48	90.62	52.22	66.26	92.32	93.20	92.76	98.01	93.25	95.57	82.31
Reformer	(2021)	82.58	69.24	75.32	85.51	83.31	84.40	90.91	57.44	70.40	72.50	96.53	82.80	59.93	95.38	73.61	77.31
Informer	(2021)	86.60	77.23	81.65	81.77	86.48	84.06	90.11	57.13	69.92	70.29	96.75	81.43	64.27	96.33	77.10	78.83
Anomaly*	(2021)	88.91	82.23	85.49	79.61	87.37	83.31	91.85	58.11	71.18	72.51	97.32	83.10	68.35	94.72	79.40	80.50
Pyraformer	(2021)	85.61	80.61	83.04	83.81	85.93	84.86	92.54	57.71	71.09	87.92	96.00	91.78	71/67	96.02	82.08	82.57
Autoformer	(2021)	88.06	82.35	85.11	77.27	80.92	79.05	90.40	58.62	71.12	89.85	95.81	92.74	99.08	88.15	93.29	84.26
Stationary	(2022b)	88.33	81.21	84.62	68.55	89.14	77.50	89.37	59.02	71.09	68.03	96.75	79.88	97.82	96.76	97.29	82.08
FEDformer	(2022)	87.95	82.39	85.08	77.14	80.07	78.57	90.47	58.10	70.76	90.17	96.42	93.17	97.31	97.16	97.23	84.97
Crossformer	(2023)	83.06	76.61	79.70	84.68	83.71	84.19	92.04	55.37	69.14	88.49	93.48	90.92	97.16	89.73	93.30	83.45
PatchTST	(2022)	87.42	81.65	84.44	84.07	86.23	85.14	92.43	57.51	70.91	80.70	94.43	87.24	98.87	93.99	96.37	84.82
ModernTCN	(2024)	87.86	83.85	85.81	83.94	85.93	84.92	95.17	57.69	71.26	91.83	95.98	93.86	98.09	96.38	97.23	86.62
TVNet	(Ours)	88.03	83.49	85.75	83.91	86.47	85.16	92.94	58.26	71.64	91.26	96.33	93.72	98.30	96.76	97.53	**86.76**

H SHOWCASES

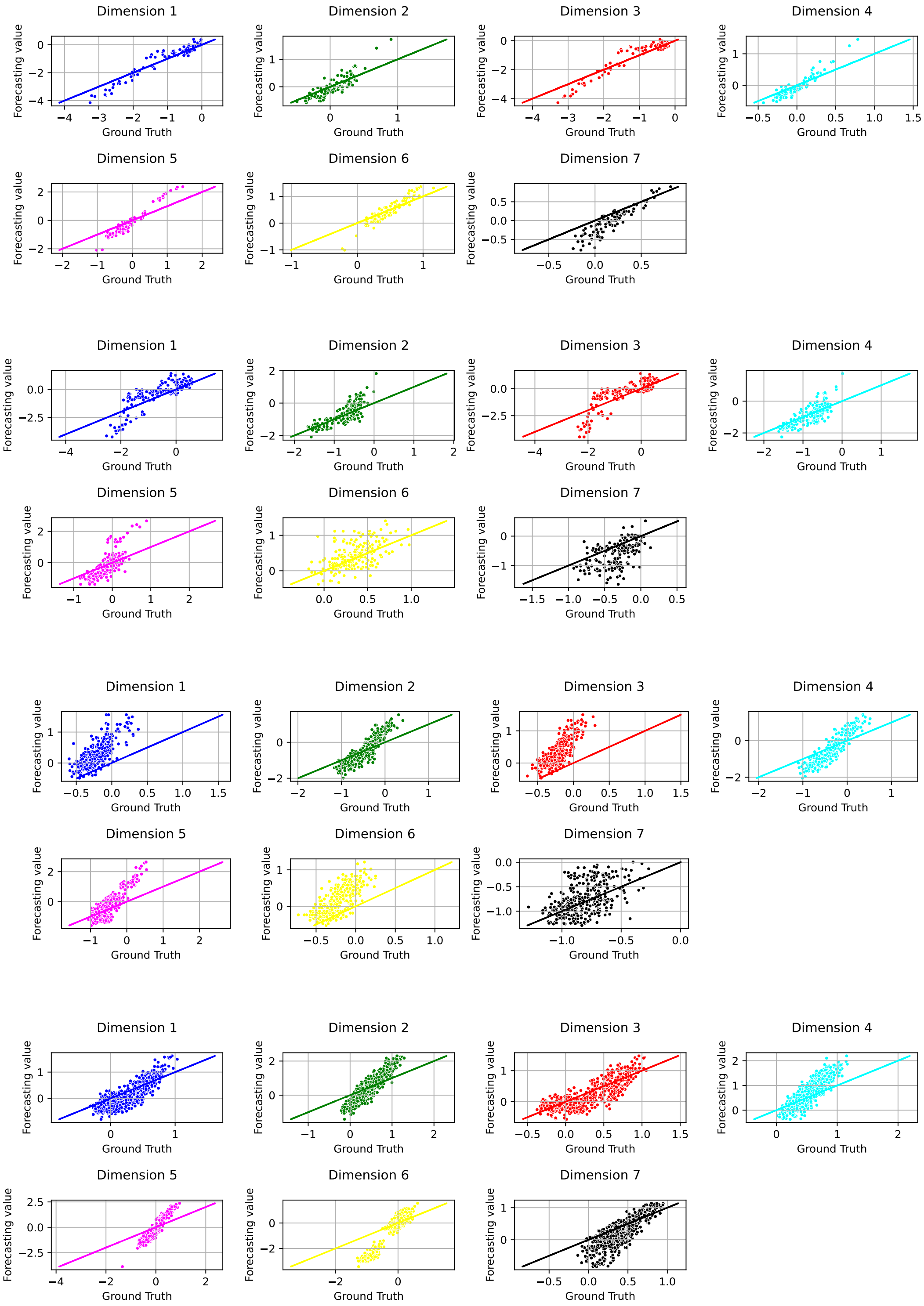

Figure 18: Visualization of ETTh1 Multivariate forecasting results

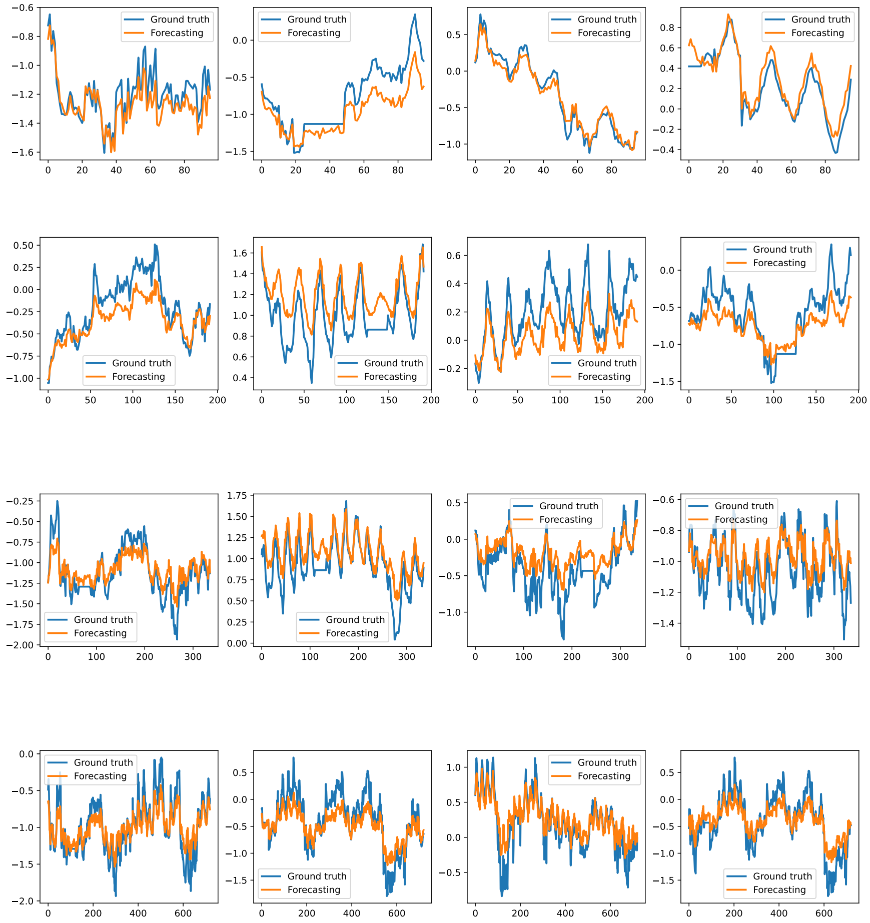

Figure 19: Visualization of ETTh1 Univariate forecasting results